THE GRAVITY FIELD AND TECTONIC SETTING OF THE GEDAMSSA CALDERA AND ITS ADJACENT AREAS.

By

Mengistu Zeleke

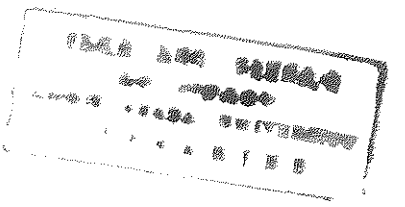

A Thesis

submitted to the

School of Graduate Studies

Addis Ababa University

In Partial Fulfillment of

the Requirements for the Degree

Master of Science in Geophysics

May 1999

ABSTRACT

In this thesis work analysis of 587 gravity data collected in the central part of the Main Ethiopian Rift (MER), between latitudes 8.00- 8.75N & longitudes 38.75- 39.5E (consisting of Gedamssa caldera is made). The data sets incorporate 50 gravity observations that are recently collected by the author with his principal advisor & the remaining 537 gravity observations obtained from previous surveys carried out by EIGS & Geophysical Observatory of A.A.U.

The analysis include compilation in a standard format of the recent & and the previous gravity data sets, which require homogenisation to IGSN71 Datum of the data set from the previous surveys that is found out not available to this datum.

All available data, about 587 stations, obtained from the EIGS and partly collected by the author, were reduced to sea level with a uniform crustal density of 2.67 gm/cm^3. Effects Bouguer masses were calculated applying the simple Bouguer correction. Terrain correction of majority of the datas was not applied in which case its effect was treated as systematic error in computing the over all mean square error of the simple Bouguer anomalies at each station. Theoretical gravity field was computed by means of the international gravity formula of 1967 (GRS67) and tied to the IGSN71. The accuracy of the Bouguer anomaly at each station is calculated to about ± 2.8 mGal. The regional and residual gravity field were calculated from the Bouguer anomaly map by means of a software that uses Hanning filter.

The compiled Bouguer anomaly map shows a strong correlation between the regional pattern and topographic feature of the survey area. Owing to higher elevations, the adjacent plateaus are marked by negative Bouguer anomalies, the minimum of magnitude -245 mGals being located around Areb gebya. The maximum gravity values occur in the NE corresponding to the relatively

lower elevations. The main Ethiopian rift including Afar is characterised by a relatively positive anomaly as compared to the plateaus. The high on the rift accounts for the excess mass at depth on which the crust lies relative to the plateaus where a mass deficiency is assumed.

Gravity values on the main Ethiopian rift are generally less as compared to the north part of the Ethiopian rift. This accounts for the thinning of crust material towards the Afar along the rift, or it can equally be explained as by a thickening of a denser material beneath the crust(probably the anomalous mantle). The margins separating the rift from the plateaus are marked by steep gravity gradients which their magnitude represent the slope of the escarpment. Steep gradients indicate the transition of gravity field from the plateaus to the rift floor.

ACKNOWLEDGEMENT

First & foremost I should offer my thanks to the One Who is a Lord of all for my successful completion of the post graduate studies. I have no words to say about my supervisor **Dr. Abera Alemu**, he is my brother, friend, and teacher. I have really benefited from his publications and his unfailing effort, talent in the field, and computer usage to bring this thesis its present final stage. Directly or indirectly he was guiding me to the right paths of both the academic and social lives. Now, I feel self confident to do research on my own in gravity (geophysics) with little or no assistance if I am given the chance. I am also deeply indebted for his support in using his personal invaluable geophysical materials, books & computer at home.

My deep heart acknowledgment to my **CO-advisor Dr. Solomon Tadesse** for his concern, encouragement and proper advice through out the progress of this research. Especially he made reliable comments and arrangements on the geological aspect of the study area. Beside this, it was not possible to bring an end this thesis with out his effort in finding financial support assisting the field expense. The Aquatech pvt.L.company and the company General Manager **Ato Girum Lisanu** acknowledged for the financial support

I was free to use all the available resources of the department including personnel assistance of the department members when I am in need of them at all times. Especial thanks goes to **Dr. Bekele Abebe** for his permission to use all his office facilities including the computer at all times in his absence and presence. I acknowledge **Dr. Tesfaye Korme** for his invaluable assistance in all my problems including the proper guidance in computer usage throughout the progress of my work.

I acknowledge all the members the Geophysical Observatory of A.A.U. in particular the Director **Dr. Lakiemariam Asefaw** for his permission to use the computer facility. Especially I am

indebted to **Dr. Atalay Ayele** & **Ato Mulugeta Tuji** for their help during my work in the proper usage of the computer.

The Ethiopian Institute of Geological Survey acknowledged for the data provided to this research work and for the use of Geosoft in the Geophysics Department. I am indebted to all members of the geophysics department for their invaluable assistance. Special thanks to **Ato Biniam & Ato Kimemu** for their friendly and invaluable assistance in using the soft ware programs to prepare the gravity anomaly maps. The help of my friends Senay, Getachew, Euyel, & Teshome are unforgettable during my stay of post graduate studies.

I owe to my mother **W/o Lackech Getahun** for her moral and spiritual support at all times. Last but not least I am indebted to my wife **Yirbebu Tarekegne** & childeren **Mekdes**, **Amanuel Mengistu** for their patience to stay along without my near help.

TABLE OF CONTENTS Pages

TABLE OF CONTENTS PAGES

TABLE OF CONTENTS PAGES

List of Figures Pages

CHAPTER 1

INTRODUCTION

1.1 LOCATION

The study area (Fig.1) is located in the central sector of the Main Ethiopian Rift (MER) considerably close to the Eastern rift margin within 38.75^0 and 39.50^0 longitude & 8.00^0 & 8.75^0 latitude.

The gedamssa caldera consisted in the study area is located about 25km south-west of Nazret town & east of lake koka.

This caldera is a large volcanic depression and has a circular dimension of about 8km in diameter and with the rims at places reaching a maximum altitude of 1950m above sea level. It has an almost flat floor, slightly tilted to the north, with elevation ranging between 1740 and 1630m above sea level, and the central part is occupied by an E-W running irregular chain of hills, locally named Ittisa, which results from presence of several volcanic edifices. One of these volcanoes, sited at the eastern edge of the chain, contain an explosion crater (Kore) being perfectly preserved with a diameter of about 1km and an average depth of about 100m. The rim of the caldera is well preserved in three sides with vertical inside walls of 100- 200m high. Only a small section of the NW rim is not recognised.

1.2.Purpose & overview of the study

Ethiopia is identified with three physiographic regions: the Western plateau, the Ethiopian Rift system and the Eastern plateau. The Ethiopian Rift system has three sectors: the Afar Depression, the Main Ethiopian Rift (MER) and the Rift system of Southern Ethiopia (Moore and Davidson, 1978). The rift system forms one of the major continental rift valleys. Almost all earthquakes and recent volcanic activities in Ethiopia are visibly associated with the rift structure and parts of the plateaus. On the other hand, there are no satisfactory geo dynamic models that can explain these and other related phenomena. The lack of sound geodynamic concept in turn hampers the understanding of the causes of earthquakes, volcanic activities, mineral exploration and energy resources development in continental rift systems like that of the Ethiopian Rift system. Apart from this the existing problem regarding the previously acquired gravity data in the country is lack of homogeneity with respect to datum & reference system adopted by different agencies involved in the reduction of their observations (hopping that the observations are correctly made following standard procedures).This problem can be evidently seen by the variation in intensity of the already generated gravity anomaly maps of the same area by the different agencies. Thus, this M.Sc research is concerned with the contribution of gravimetric solutions to these problems by compiling all the available previous gravity data & data collected under this survey in a standard format & make it readily available for interpretation work in connection to finding solutions to the problem sited above.

The main objectives of this thesis therefore are:

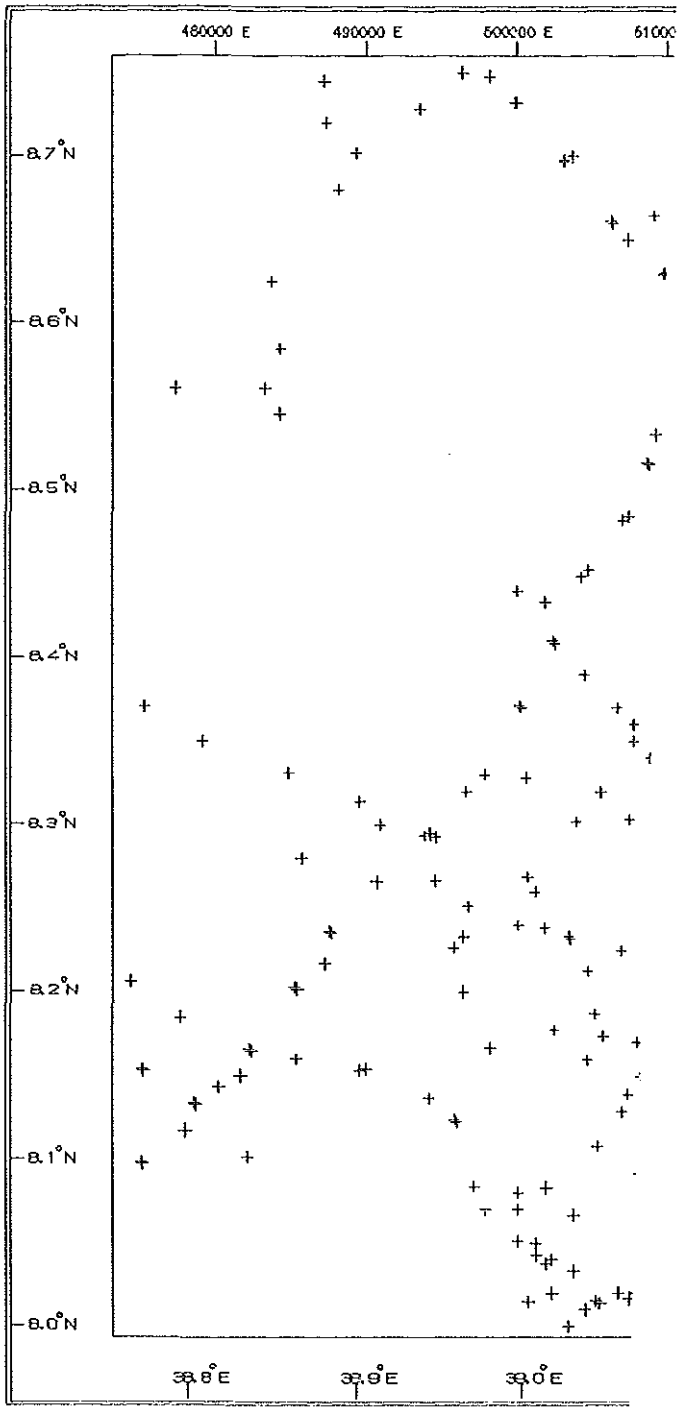

Fig.2 DATA LOCATION POINTS IN GEDEMSA AND ITS

compile the previous data obtained from the involved agencies like EIGS,A.A.U. & the data acquired under this survey with a homogenisation to the same datum (IGSN71 Datum) & reference system (GRS 1967).

-generate anomaly maps of the study area with the homogenised version of the compiled data set.

make a preliminary qualitative interpretation of the gravity

anomaly pattern (distribution, location, and orientation of gravity anomalies) resulting from the compiled gravity anomaly maps in terms of variations in density of near surface and sub-surface geological bodies residing beneath the study area.

- compare the results (gravity anomalies and anomaly maps) of the homogenised data set with that of its earlier version (i.e., obtained from the agencies mentioned and found out to be heterogeneous).

This thesis describes the results of 587 gravity observations made in the study area so far and compiled in accord with the objectives cited above.

The generated anomaly maps are found out to give a first hand reliable information in the distribution, location and orientation of the geological structures of the area that is consistent with field observations and indicated on the geological map of the area. Moreover, the compiled data is believed to contribute a bit to the national challenge in the compilation of a homogenised gravity data catalogue of the country.

The thesis is organised in six chapters. The first chapter is introduction to the thesis. The second & third chapters discus the previous geological & geophysical works of the study area.. The fourth chapter addresses the theoretical basis of gravity study. In the fifth chapter, a discussion on the field work, data reduction, assessment of the associated errors, compilation

of the Bouguer anomaly map and a qualitative description of the observed Bouguer anomalies is presented. The last chapter is conclusion & recommendation.

CHAPTER 2

GEOLOGICAL AND TECTONIC REVIEW

2.1. GEOLOGIC AND TECTONIC SETTING OF THE ETHIOPIAN RIFT SYSTEM

The Ethiopian rift system is claimed to consist of three distinct segments. These from north to south are the Afar depression, the Main Ethiopian Rift (MER) and the Southern Ethiopian Rifts (SER).

A summary of the geology of an area is regard as a necessary background for a gravity interpretation and discussion. Hence, a brief discussion of the surface geology and fault structure determined from surface observations carried out in the Main Ethiopian Rift are presented.

Since the initial work of Mohr (1960), the geological history of this region has been documented by several authors (Mohr, 1960, 1962a&b, 1967, 1972 and 1983; DI Paola, 1972; Ljoyd, 1977; Baker et al., 1972).All the geological and structural descriptions that will be considered here as relevant to this study are summarised from these previous studies.

The Ethiopian Rift system is the northern most extension of the great East African Rift that extends from northern Ethiopia to Mozambique in southern Africa, a distance of more than 4000 km. More than one quarter of the great East African Rift lies in Ethiopia.

The Rift bisects the highlands of the country into the Eastern and Western highlands and the floor of the Rift Valley is commonly at an elevation of about 1000 m less than the adjacent highlands.

The highlands are commonly underlain by Tertiary plateau type flood basalt and rhyolite while the floor of the rift is commonly Quaternary to Recent basin fill sediments, alluvium and young volcanic products. In some areas, the Rift escarpment is highly pronounced while others are more gradual, as the result of a series of step faults down-thrown into the graben.

At the northern end of the Main Ethiopian Rift (MER), an area referred to as the Afar Depression, the rift Valley becomes extremely broad, up to 250 km wide due to the fact that it is the focus of a continental plate triple junction (Afar Triple Junction). The three major tectonic lineaments that dominate the structure in this part of the Rift are the Red Sea Trend (a NW-SE trend), the Gulf of Aden Trend (roughly an E-W trend), and the Ethiopian Rift Trend (a NE-SW trend).

Volcanism appears to be more basic and younger to the north-east, although young volcanism is also common throughout the entire Ethiopian Rift. The internal grabens of the Afar depression are filled with Quaternary to Recent basin fill sediments, rhyolite domes, fissure basalt flows, numerous cinder cones and basaltic to peralkaline rhyolitic volcanoes.

The Main Ethiopian Rift (MER) is a half graben with an average width of about 70-80 km and a length of some 700 km stretching NNE from the southern boarder, to its northern end where it joins the Afar triangle. It lies between latitude 5 - 9 N and longitude 37 30' - 40 E. The eastern escarpment is characterised by step faults with significant throw in its NE sector exceeding 1500 m between the top of the plateau to the rift floor. The western margin is gradational and less marked accounting for the asymmetry of the MER. Tectonic movements are still active in the MER, as confirmed by the numerous young faults often affecting Holocene rock units and by the intense seismicity of the whole region.

The main petrological feature of the MER is the abundance of silicic peralkaline volcanics (mainly pantallerites) related both to the fissural activity and to the several central volcanoes rising from the rift floor. It is considered that east-west tectonics may be an important factor controlling the locations of volcanic and volcano-sedimentary products that are devoid of both marine sediments and crystalline rocks. Sediments of lacustrine origin are well represented; they cover large areas of the rift with sometimes great thickness.

The volcanic rocks along the boundary faults of the northern sector of the MER range from Oligocene to Pliocene (28 - 5 Ma). A single date of 27.8 Ma and Plio-Pleistocene dates (5.3 - 1.2 Ma) were reported from the rift margins and shoulders of the central sector of the MER (Mohr and Potter, 1976; Merla et al., 1979). Like the northern sector, the boundary faults of the southern sector of the MER expose Oligocene to Miocene (31.7 - 11.9 Ma) volcanic rocks (Zanettin et al., 1978). The central volcanoes within the rift belong to Late Quaternary volcanic facies, younger than 0.8 Ma.

2.2 Geological review of the study areas

Reconnaissance study covering the central sector of the Main Ethiopian Rift valley was conducted since early 1996. One of the major areas promoted for detailed investigation is the Gedemsa caldera situated at the intersections between the MER tectonic trend (NNE-SSW) and incipient transverse lineaments (E-W). The central volcano fall along incipient EW transform fault that mark the southern and northern ends of the MER. The volcanological history of the caldera features is attributed to central type eruptions, with subsequent volcano-tectonic collapses.

The Gedemsa volcano is a recent (0.8 to 0.1 Ma) volcanoes in the central sector of the MER. It is built up of acid lavas and pyroclastics and is characterised by a polgenic caldera resulting from large pyroclastic eruptions. The lowest exposed products are represented by acidic lavas, which are covered by thick plinian fall pumice deposits. These are followed by an ignimbrite deposit and by intra-caldera lava and inter- bedded pyroclastic products. The caldera is clearly a composite structure resulted from several collapse which occurred as a consequence of plinian and ignimbritic eruptions. The volcanic products of Gedemsa consist mainly of peralkaline trachytes and rhyolites, mafic rocks being represented only by inclusion occurring within some of the post-calderic products.

The whole caldera is strongly affected by many large regional NNE-SSW faults, especially on its eastern part.

There are evidences that indicates past hydrothermal activity in the north-west rim and on a small dome inside the caldera. Occurrences of several active thermal manifestations are also known along NNE fault lines immediately outside the caldera proper. The ancient manifestations have oxidised pumiceous deposits with some deposition of silica. Two geothermal wells have been drilled within the Gedemsa caldera to depths of 190 and 200 meters with rock cutting samples taken every 3 meters.

2.3. STRATIGRAPHIC OUTLINE OF THE ETHIOPIAN RIFT VALLEY.

This part of the Ethiopian rift valley is exclusively made up of volcanics and volcano sedimentary products, with neither marine sediments or crystalline rocks. Sediments of lacustrine origin are well represented; they cover large areas of the rift with sometimes great thickness.

The successive periods of volcanic activity in this part of the rift valley the following main events.

-Fissure eruptions with emplacement of explosive dominantly ignimbritic products followed by volcano-tectonic collapses;

-Building of silicic central volcanoes;

-Basaltic fissure eruptions;

-Edification of recent mostly pantelleritic centers with associated "en echelon" basaltic fissure eruptions.

As a result of the above processes the stratigraphic succession of the area may be reconstructed as follows.

Aluvium	Recent plestiocene
recent alkaline and peralkaline rhyolitic pumice, ashes and obsidian lava flows	Holocene
alkali trachaytic lava	Recent pliocene
recent basaltic lava flows and spatter cones	Recent pleistocene
basaltic hayallo clastites	Recent plestiocene
old alkaline and peralkaline	Early pleistocene

rhyolitic lava flows and domes associated to pumice and ashes	Late pliocene
alkaline and ;peralkaline ignimbrites associated to pumice, ashes and lahars (mud flows)	Pliocene Early Eocene

2.4. THE GADAMSSA CALDERA

It is one of the central volcanoes found in this part of the Ethiopian rift valley. The Gedamssa volcano is located in the central sector of the Ethiopian rift valley about 25km south west of Nazret town considerably close to the eastern rift margin . The study area which includes the caldera lies within 39 6E and 39 14E longitiude and 8 17N and 8 28N latitude. The area is bounded to the north by Awash river, to the west by the Koka lake and to the east by Wonji sugar plantation.

This caldera is adjacent to the Wonji sugar estates farm SW boundary. It is almost perfectly circular with diameter of about 8(10)km. The rim of the caldera is well preserved with vertical inside walls of about 100-200m high.

Only a small section of the NW rim has been eroded. The rocks which form the rim of the caldera are mostly rhyolitic lavas, even though pumice and ignimbrites are rather abundant.

The north- eastern rim of the caldera is formed by some very thick (20-30m) rhyolitic lava flows, showing a clear flow age folding. In some places, coarse explosion breccias made up hetrogeneous volcanic material, lie at the base of the lava flows. The lava is covered and interbeded with finely bedded pyroclastic materials (small pumice, minute salic crystals, ashes) dipping, as the lava flows, towards the wonji plane. The interior of the caldera shows several signs of post- caldera activity. Some small dome-like features occur mostly consisting of pumice falls with subordinate rhyolitic lavas. The most important feature is an irregular chain of hills rising for about 200-250m from the floor of the caldera. It is made up of alteration of rhyolitic lavas and pumice deposits.

This chain is locally named Itissa and, on its eastern part, there is a large crater with a diameter of about 1km and a depth of about 100m. A large amount of underlying formations is found as blocks within the pumice deposits and as xenoliths in the lavas inside the Itissa crater. The most abundant inclusions are represented by a strongly porphyritic basalt, which, as previously mentioned, outcrops in this area. The whole caldera is strongly affected by many large regional NNE-SSW faults, especially on its eastern part. Along one of these faults, close to the inside NE rim of the caldera, a small basaltic spatter cone was built; at present, the spatter cone shows vertical and dextral dislocations due to a later movement of the same fault. Another small basaltic spatter cone is located close to the western inside rim of the caldera. Weak traces of fumarolic activity are visible at the base of the western rim of the caldera and on a small pumice dome on the west.

2..5 STRATIGRAPHY & VOLCANOLOGY OF THE GEDAMSSA VOLCANO

General and previous investigations.

The Gedamssa volcano is found in extensional tectonic setting in rift where voluminous volcanism occurs. The volcanic history of the center has been dominated by the eruptions, in the form of both lavas and pyroclastics, of silicic magmas.

The lowest exposed products are represented by acidic lavas, which are covered by thick plinian fall pumice deposits. These are followed by an ignimbrite deposit and intra-caldera lava flows and inter-bedded pyroclastic products. The formation of the caldera, is clearly a composite structure resulting from the occurrence of several collapses. A separate stage of volcanic activity (basaltic volcanism) formed surge deposits and numerous basaltic cinder cones and lavas, both within and outside the caldera depression. Interbeded oxidised soil horizons(red boles) occur in several places within the volcanic sequence and record repose periods between eruptions.

In the Gedamssa caldera, extensive sediment successions developed within and outside the depression. These are typical continental sediments (fluvial, aluvial fan and lacustrine).

From the knowledge of the stratigraphy, it is clear that eruptions from the rhyolitic centers of Gedamssa are separated by relatively long repose period. On the other hand, the basaltic volcanoes show a common progression from phreato magmatic to strombolian phase. This reflects a decrease in the water-magma interaction during the eruption.

A primary account on the geology of the Gedamssa caldera has already given by a few author. Diapola(1972) mentioned briefly the geology of some of the major units of the center and showed the presence of dextral dislocation associated with the normal movement.

Thrall (1973) described and classified the volcanic products on the basis of the field characteristics and analytical (major element) data. According to Thrall the caldera collapse

was not associated with outpourings of ignimbrite or pumice fall out collapse was caused by foundering of a large part of the cone along a cylindrical fault.

A geo-volcanological investigation on Gedamssa was carried out as part of an epitermal reconaissance study of the selected sites of the Ethiopian rift system by EIGS and ELC(1987). They suggested that the caldera was formed through ignimbritic eruptions and attributed a phreato magmatic origin to the Kore crater.

Recently, Damte (1990) provided a valuable account on the volcano tectonic features of the volcano. He presented a generalised stratigraphy of Gedamssa volcano which starts with abase of very thick pyroclastic flow and ignimbrites followed by rhyolites and obsidian lava flows of post caldera activity capped finally by pumice fall deposits.

2..6. STRUCTURAL & VOLCANOLGICALOUTLINESOFGEDAMSSA CALDERA

Gedamssa volcano morphology is dominated by a circular caldera, about 8km(10km) in diameter and minimum NNW elongation. Thus the shape of the caldera does not reflect the regional stress patterns and is purely the result of magmatic activities. The shallowest part of the structure occurs in the Northeast. The central part of the caldera is occupied by cones and domes which rich an altitude of about 200m with respect to the caldera floor. There is no evidence for the occurrence of resurgent structures (i.e. later up doming of the intracalderlic ignimbrite or sediments). The altitude of the caldera rim is very uneven with a maximum of 1950m on the west and maximum altitude difference with respect to the caldera floor of about 250m. This suggests the occurrence of several pre-caldera flows and domes along the flank of

the volcano. The Northeast part of the caldera is characterised by a younger escarpment and by a more depressed calderic floor. This suggests that the caldera has been formed by several eruptions and the most recent collapse occurred in the Northeast. Linque et al(1991) suggested that the caldera collapse occurred in two phases.

Field observations confirmed a two phase collapse for the caldera. The first phase occurred as a consequence of huge plinian explosive eruptions which prosuced the lower pumice fallout deposits which are by far the most wide spread pyroclastic unit of the Gedamssa volcano, being found over wide areas both inside and outside the caldera. The second phase of caldera formation was connected with the ignimbritc eruption and mainly affected the northern and north-eastern part of the previously formed structure(Derje,1994).

Analysis of satellite images indicate that an older caldera almost completely covered by younger products is present just north of the Gedamssa volcano. The southern rim of this older caldera intersects the Northeast edge of the Gedamssa caldera and its presence has strong effects on the geometry of the collapse connected to the ignimbrite eruption. Indeed, this explains why the northern edge of the Gedamssa caldera shows a convexity rather than a concavity towards the center of the depression.

CHAPTER 3

3.1. PREVIOUS GEOPHYSICAL STUDIES AND RESULTS

The whole area of potential interest, covering an area of about 200km^2 and centred about the Gedemsa caldera, has been covered with an adequate density by the geoelectrical and gravimetric surveys. The combination of the results contributed in clarifying the stratigraphic and structural setting of the area. The following stratigraphic sequence can be hypothesised (starting from the youngest formation).

-aluvium and recent basaltic flows (thickness up to 100m),

-post caldera pumice and rhyolites, only present inside the caldera and west of it (thicknesS of up to 300m),

-pre-caldera rhyolites, presumably extending with a tabular shape all over the area of interest(average thickness of 200m),ignimbrites mainly attributable to the Nazret group (thickness usually included between 500 and 800m),basalts of the rift floor constituting the basement of the area.

The ignimbrites represent the conductive unit having a resistivity of 15 to 40Ωm inside the caldera and 5to 15Ωm outside of it (Electro consult and EIGS report,1987).The other formations have a resistivity from medium to high, except for the aluvium which is conductive

CHAPTER 4

4. BASIC THEORY OF GRAVIMETRY

A theoretical treatment of the subject given in this chapter is compiled from lecture notes of the post graduate course gravity and magnetic methods delivered by Dr. Abera Alemu at the department of Geology & Geophysics at A.A.U.& the standard text book in Geophysics (Telford,et al,.1990, Dobrin& Savit,1988, Turcotte et al., 1982 ..., etc.)

4.1 Gravity and Gravimetry.

Gravity and magnetic fields are two natural force fields interact to the earth. This is because the Earth has the ability to attract material masses towards its center. The gravity field is always an attractive force.

The Earth also attracts or repels material masses which have a magnetic properly. This a simple evidence for the Earth to have a magnetic properly (Telford, et al., 1990).

How do we model the attractive force mathematically?

The reason why they are attracting still unknown scientifically but it is observed that the two bodies are attracting each other. The fundamental principle on which the gravity method based is the Newton s law of universal gravitation. It states that every particle of matter exerts a force of attraction on every other particle this force being directly proportional to the product of the masses and inversely proportional to the square of the distance between them.

$$\mathbf{F = Gm_1m_2 / r^2} \qquad \mathbf{(4.1)}$$

where F - is the mutual gravitational mass attraction of the two particles of masses m_1 and m_2.

r -is their separation distance.

and G- is the universal gravitational constant which has a value equal to 6.672X10-11 m^3 kg^{-1} in SI unit.

One of these entities can be considered as an external force. For example the force of attraction by m_2 on m, can be considered as an external force to m, that causes a change of state.

$$F = Gm_1 m_2/ r^2 = m_1 a_1$$

$$\text{or } F = Gm_1m_2/r^2 = m_2a_2$$

Typical example- A mass [m] above the Earth.

$$\mathbf{F = G\ Mm/\ r^2 = mg} \qquad \mathbf{(4.2)}$$

is the external force causing m to accelerate.

$$F/m = GM/r^2 = g$$

is known as the gravity field [gravity field intensity] or intensity of gravity acceleration.

GRAVITY: is the force per unit mass to accelerate the mass m on the surface or exterior to the surface of the Earth. Gravity field can have components along x, y, and z axes. In this case we call it gradient of gravity field.

$$\mathbf{grad}\ g = \nabla g = \delta g/\delta x + \delta g/\delta y + \delta g/\delta z$$

4.2. What is Gravimetry?

By Gravimetry {Latin: Gravis = heavy; Greek: metry =to measure} is a method of measuring and representing [modelling] the gravity field of the Earth[g](Torge, 1989].

Important in measuring the gravity field of the Earth is that:

It is position dependent. I.e. "g" varies from place to place. g = g[{x-y}, z] in plane co-ordinates, where x-y represents latitude and longitude, and z height. g = g{r., θ, ϕ } in spherical co-ordinates.

Gravity can also be affected by the extension of other terrestrial masses {extra terrestrial masses}and by the rotation.

Modelling Gravity [Gravity force per unit mass acting on a mass m on Earth].

$$g_m = GM/r^2 \qquad (4.3)$$

Unit of " g " in Geodesy is Gal [G] given in the honour of Gallileo Gallili.

$$1\ \text{Gal} = 1\text{cm/s}^2 = 10^3\ \text{mGal}.$$

Gravity unit (g.u)

$$1\ \text{g.u} = 0.1\ \text{mGal},\ 1\ \text{Gal} = 10^3\text{mGal}$$

The units tell you the accuracy of determination. The smallest unit has more precision than the big unit.

4.3 Factors affecting the gravity field.

Consider a small mass moving with a velocity v on the surface of the Earth rotating with angular velocity ω as shown below (Fig.4.3)

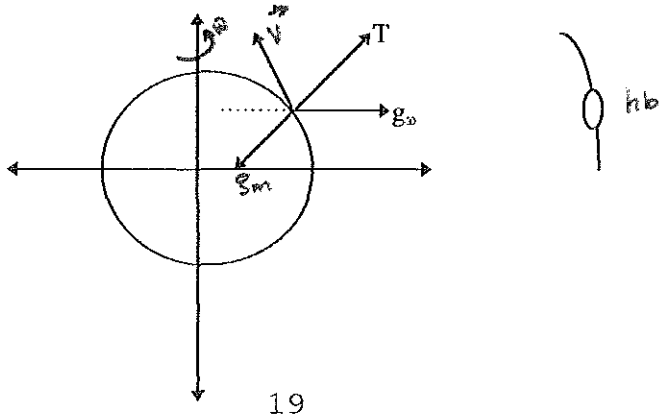

Fig.4.3 Force components affecting g_m

The possible force acting on a body of mass m moving with a velocity v on the surface of spherical Earth of radius R rotating with angular velocity w are [Heiskanan and Mortiz, 1967]

$$g = g_m + g_\omega + c + T \quad \text{and is known as gravity.}$$

where, g_m - is the attraction force per unit mass acting on m due to Earth's mass.

g_ω - is the centrifugal force per unit mass acting on m due to Earth' s rotation with ω.

C- is the coriolis force per unit mass acting on m due to its motion with linear velocity v on the surface of the Earth.

T-is the tidal force per unit mass acting on m due to mass attraction of other heavenly bodies.

For spherical model of the Earth with radius R:

$$g_m = GM/R^2;\ g_\omega = \omega\,[\omega \times R],\quad F_\omega = m\omega[\omega \times R] \qquad (4.4)$$

$C = 2[\omega \times v]$; $C = 0$ if $v = 0$ or if m is at rest on the surface of the Earth.

It is not easy to express T with a simple formula due to the variation in position [as they are always rotating their position change with respect to position of m] and a number of heavenly bodies causing it.

The effect of C and T on g is usually considered negligible in actual work. Gravity, g refers to the combined effect of both Earth' s mass gravitation and rotation [centrifugal acceleration] .i.e.

$$g = g_m + g_\omega$$

$$\mathbf{g = GM/ R^2 + \omega[\omega \times R]} \qquad \textbf{(4.5)}$$

4.4Centrifugal acceleration and acceleration of gravity for a spherical Earth model.

Inertial co-ordinate system: is used to express the motion of a planetary bodies around the Sun. In this co-ordinate system F = ma [Newton' s 2nd law] is valid and ω can also be expressed in this co-ordinate system. But the global variation of g is valid on Earth fixed

Geocentric co-ordinate system. This co-ordinate is used to determine the global variation of "g" on the surface of the Earth.

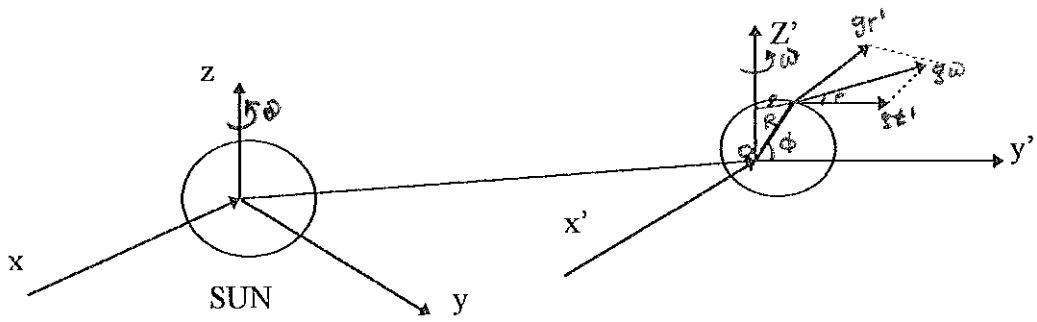

Fig.4.4 Figure of the Earth

From the figure:

$g_r = g_\omega \cos \phi$ is the radial component .

$g_t = g_\omega \sin \phi$ is the tangential component.

g_r has no any influence on the mass attraction [g_m]. It is only g_r has effect on the mass attraction. This is always to reduce g_m.

Earth fixed -geocentric co-ordinate system.

used for the global representation of the gravity field [g].

-its origin is the Earth' s center of gravity.

- the Earth and every thing fixed to its surface is acted by the same centrifugal acceleration [g_w].

- g_ω points out radially outward along a line perpendicular to the rotation axis and S is perpendicular to the rotation axis ω.

$$g_\omega = \omega^2 S, \qquad S = R\cos\phi$$

$$g_\omega = \omega^2 R\cos\phi$$

$$g_r = g_w \cos\phi = \omega^2 R\,COS^2\phi \qquad (4.6)$$

$$g_t = g_w \sin\phi = \omega^2 R\cos\phi\sin\phi,$$

Let gm -is directed radially inward be positive and gr -is directed radially outward be negative.

$$\mathbf{g = g_m - g_r = g_m - \omega^2 R\cos^2\phi} \qquad \mathbf{(4.7)}$$

Thus g_r reduces the gravity by an amount $\omega^2 R\cos^2\phi$ .At the Equator $\phi = 0$ and at the poles $\phi = \pm 90$.

$g_r = \omega^2 R \cos^2 0 = \omega^2 R$ is maximum at the Equator.

$g_r = \omega^2 R \cos^2 90 = 0$ is minimum at the poles.

$g_E = g_m - g_r = GM/R^2 - \omega^2 R$ is minimum

$g_p = g_m - g_r = GM/R^2 - 0 = GM/R^2$ is maximum

The Gravity - gr field difference at the poles and the equator is given by;.

$$g_p - g_e = \omega^2 R = 3.4 \text{ Gals}$$

for a spherical symmetry Earth of radius R = 6.4 x 103km and ω in rad/sec. For the real Earth, observed values [pendulum observations] of g at the poles and equator are;

g_p =983.218Gals, g_e =978.032Gals

From the observed value $g_p - g_e$ = 5.2Gals, which is different from the theoretically computed value for a spherical symmetric Earth - model. Hence the disagreement between the observed and calculated values of 'g' indicates:

1. The shape of the real Earth is not spherical as it was assumed.

2. The shape of the Earth is a rotationally distorted one such that its shape is flattened at the poles and bulged at the equator.

3. g varies as a function of latitude as observed above.

4.5 Gravitational acceleration to the rotationally distorted Earth:

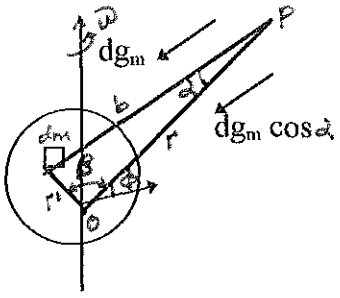

Fig.4.5 Attraction, centrifugal force and gravity on spherical Earth

From the fig. we can establish the following relations.

1. $\cos\alpha = (b^2 + r^2 + r'^2)/2rb$ - cosine law.
2. $dg_m = Gd_m / b^2$
3. The component of the gravity acceleration along the line from p to o is $G \cos\alpha\, d_m / b^2$
4. $g_m = G \int (\cos\alpha / b^2)\, dm$

Using "1" in 4 we have:

$$g_m = G/2r^2 \int [\, r^3/b^3 + r/b - r'^2 r/b^3 \,]\, dm$$

$$= G/2r^2 \int [\, r/b + r^3/b^3 \{\, 1 - r'^2/r^2 \,\} \,]\, dm$$

5. $b^2 = r^2 + r'^2 - 2rr' \cos\beta$ - cosine law.

6. $b^2 = r^2 / b^2 = r^2 / [\, r^2 + r - 2\, rr' \cos\beta]$

$$r/b = [1 + r'^2/r^2 - 2(r'/r)\cos\beta]^{1/2}$$

Substituting the final expression of 6 into 4 we have:

$$g_m = G/2r^2 \int [\, \{1 + r'^2/r^2 - 2(r'/r)\cos\beta\}^{-1/2} +$$

$$\{1 + r'^2/r^2 - 2(r'/r)\cos\beta\}^{-3/2} \{1 - r'^2/r^2\} \,]\, dm$$

$$g_m = G/2r^2 \int \{1 + r'^2/r^2 - 2(r'/r)\cos\beta\}^{-1/2}$$

$$[1 + \{1 + r'^2/r^2 - 2(r'/r)\cos\beta\}^{-1} \{1 - r'^2/r^2\}] \qquad (6.1)$$

Using power series expansion and retain terms up to $\{r'/r\}^2$ only:

$$\{1 + E\}^{-1/2} = 1 - E/2 + 3E^2/8 + \ldots \text{ for } E<1$$

$$\{1 + E\}^{-1} = 1 - E + E^2 + \ldots \text{ for } E<1$$

Similarly we have:

$$[1 + r'^2/r^2 - 2r'/r \cos\beta]^{-1/2} = 1 - r'^2/2r^2 + (r'/r)\cos\beta + 3/2\,(r'^2/r^2)\cos^2\beta \qquad (6.2)$$

$$[\, 1 + r'^2/r^2 - 2(r'/r)\cos\beta]^{-1} = 1 - r'^2/r^2 + 2\,(r'/r)\cos\beta + (r'^2/r^2)\cos^2\beta$$

Using 6.2 £ 6.3 in 6.1 we have:

$$g_m = G/r^2 \int \{1 - r'^2/2r^2 + (r'/r)\cos\beta + 3/2\,(r'^2/r^2)\cos^2\beta\}$$

$$[1 + \{1 - r'^2/r^2 + (2r'/r)\cos\beta + 4\,(r^2/r^2)\cos^2\beta\,\{r'^2/r^2\}]dm$$

$$gm = G/r^2 \int [2 - 2r'^2/r^2 + 4\,(r'/r)\cos\beta + 4\,(r'^2/r^2)\cos^2\beta -$$

$$r'^2/r^2 + 2\,(r'^2/r^2\cos^2\beta + 3(r^2/r'^2)\cos^2\beta\,]\,dm$$

$$g_m = G/r^2 \int dm + 2G/r^3 \int r'\cos\beta\,dm + 3G/r^4 \int r'^2\,(1 - (3/2)\sin^2\beta]\,dm$$

$2G/r^3 \int r\cos\beta\,dm = 0$, since it is the first moment of the distribution. It is by definition zero if the origin of the co-ordinate system is the center of mass of the distribution.

8. $$\mathbf{g_m = GM/r^2 + 3G/r^4 \int r'^2\,[1 - (3/2)\sin^2\beta]\,dm} \qquad \mathbf{(4.8)}$$

Where GM/r^2 - is the gravity acceleration of a spherical mass distribution.

and the second term is the modification due to rotationally induced oblatness of the body.

4.5 .1. Transformation of co-ordinates.

$$r'^2 = x^2 + y'^2;\ x' = r' \sin\theta \cos\phi';\ \ y' = r' \sin\theta' \sin\phi;$$

$$z' = r' \cos\theta$$

9. $C = \int [\, X'^2 + y^2 \,]\, dm = \int r'^2 \sin^2\theta' \, [\cos^2\phi' + \sin^2\phi' \,]\, dm$

$$C = \int r'^2 \sin^2\theta' \, dm$$

is the moment if inertia about the z-axis (rotation axis) defined by $\theta = 0$degree.

10. $A = \int [y'^2 + z^2 \,]\, dm = \int r^2 [\, \sin^2\theta' \sin^2\phi' + \cos^2\theta' \,] dm$ - is the moment of inertia about x- axis defined by

$\theta = \pi/2$ and $\phi = \pi/2$

11. $B = \int [\, x'^2 + z^2 \,]\, dm = \int r'^2 [\sin^2\theta' \sin^2\phi' + \cos^2\theta'] dm$ - is the moment of inertia about y- axis defined by

$\theta = \pi/2$ and $\phi = \pi/2$.

For axial symmetry about z- axis:

$$A=B;\ A+B+C = 2A+C=2B+C$$

$$2A + C = 2\int r'^2 [\, \sin^2\theta' \sin^2\phi' + \cos^2\theta' \,]\, dm + \int r'^2 \sin^2\theta' \, dm$$

$$2A + C = \int 2r'^2 \sin^2\phi' [\sin^2\theta' + \cos^2\theta' / \sin^2\phi' + \sin^2\theta' / 2\sin^2\phi']\, dm$$

For axial symmetry about z-axis, $\theta = 0$.

$$2A+C = 2\int r'^2 dm$$

$$\Rightarrow \quad A+1/2C = \int r'^2 dm$$

Again $$\int r'^2 \sin^2\beta\, dm = \int r'^2 (1 - \cos^2\beta)\, dm$$

$$\int r'^2 \sin^2\beta\, dm = \int r'^2\, dm - \int r'^2 \cos^2\beta\, dm$$

$$= A + 1/2\, C - \int r'^2 \cos^2\beta\, dm \qquad (11.1)$$

Substituting eqn. 11.1 in eqn. 8 we have:

$$g_m = GM/r^2 + 3G/r^4 (A+ 1/2\, C) - 9G/2r^4 [A + 1/2\, C - \int r'^2 \cos^2\beta\, dm]$$

The quantity r' cos β is the projection of r' along op. This quantity can be expressed as:

$$r' \cos \beta = x' \cos \phi + z' \sin \phi$$

where ϕis the latitude or the angle between op and the xy-plane. Note that y' has no projection onto op, since op is in the xz-plane.

$$\int r'^{2} \cos^2 \beta \, dm = \int x'^{2} \cos^2 \phi \, dm + \int 2x'z' \cos \phi \sin \phi \, dm + \int z'^{2} \sin^2 \phi \, dm \quad \textbf{(A)}$$

For an axial symmetric body:

$$(x'^2+y'^2)\, dm = 1/2C \quad \textbf{(B)}$$

$$\int z'^2 \, dm = \int (x'^2+y'^2+z'^2) \, dm - \int (x'^2+y'^2) \, dm$$

$$A+1/2C = \int (x'^2+z'^2) dm + \int x'^2 dm = \int r'^2 dm$$

$$\int z^2 \, dm = A+I/2C - C = A-I/2C \quad \textbf{(C)}$$

With mass symmetry about the equatorial plane we have:

$$\int x' z' dm = \int r'^2 \cos\theta' \sin\theta' \cos\phi \, dm = 0 \qquad \textbf{(D)}$$

Using the expressions (B), (C), and (D) in (A) we have:

$$\int r'^2 \cos^2\beta \, dm = 1/2\ C \cos^2\phi + (A - 1/2\ C) \sin^2\phi \qquad \textbf{(E)}$$

From the previous expression we know that:

$$\int r'^2 \sin^2\beta \, dm = A + 1/2C - \int r'^2 \cos^2\beta \, dm \qquad \textbf{(F)}$$

Using E in F we have:

$$\int r'^2 \sin^2\beta \, dm = A + 1/2\ C - 1/2C \cos^2\phi - A\sin^2\phi + 1/2\ C \sin^2\phi$$

$$= A\cos^2\phi + C \sin^2\phi$$

Thus the expression for gm can be written as:

$$g_m = GM/r^2 + 3G/r^4 \,(A + 1/2\ C) - 3G/2r^4 \,(A\cos^2\phi + C \sin^2\phi)$$

$$g_m = GM/r^2 - 3G/2r^4\,(C - A)\,[\sin^2\phi / 2r^4 - 1] \qquad \textbf{(4.9)}$$

is the simplified form of Mac Cullagh's formula for an axis symmetric body.

The moment of inertia about the rotational axis C is larger than the moment of inertia about an equatorial axis A because of the rotational flattening of the body. It is customary to write the difference in moment of inertia as a fraction of J_2 of Ma^2 i.e.

$$C - A = J_2 Ma^2,$$

where a is the equatorial radius.

In terms of J_2 gm can be expressed as:

$$\mathbf{g = GM/r^2 --3GMa^2J_2 /2r^4 [3 \sin^2 \phi - 1]} \qquad (4.10)$$

The currently accepted values for a, GM and J_2 are:

$$a = 6378.139\text{km}, GM=3.986005 \text{ xl}0^{14}\text{m}^3\text{s}^{-2}, \text{ and}$$

$$J_2 = 1.0827 \times 10^{-3}$$

N.B. The Earth' s gravitational field can be accurately determined from the tracking of artificial satellites. Although a satellite is acted upon only by the Earth' s gravitational

acceleration, an object on the Earth s surface is also subjected to a centrifugal acceleration due to the Earth s rotation

4.6. Centrifugal acceleration and the acceleration of gravity.

The force on a unit mass at the surface of the Earth due to the rotation of the Earth with angular velocity w is the centrifugal acceleration g_w . It points out radially outward along a line perpendicular to the rotation axis and passing through p. From the (fig.4.6) below we can verify the following relations.

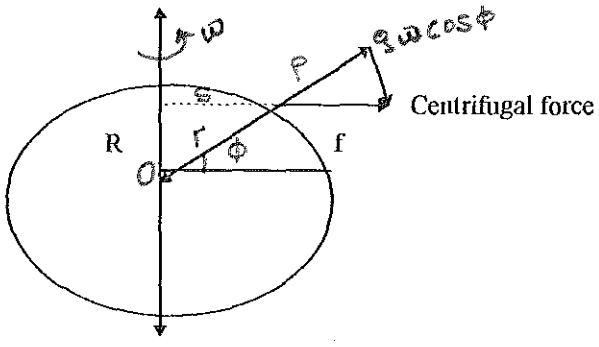

Fig.(4.6) TAHE CENTRIFUGAL FORCE DUE TO THE REVOLUTION OF THE EARTH

$$g_\omega = \omega^2 S = \omega^2 r \cos\phi \; ; \; g_r = g_w \cos\phi = \omega^2 r \cos^2\phi \; ,$$

$$g_t = g_\omega \sin\phi = \omega^2 r \cos\phi \sin\phi$$

The gravitational and centrifugal acceleration of a mass at the Earth's surface combine to yield the acceleration of gravity (g).

$$g = g_m - g_r$$

$$\mathbf{g= GM/r^2 - 3GMa^2J^2/ r^4 (3\sin^2 \phi - 1) \omega^2 r \cos^2 \phi} \qquad \mathbf{(4.\ 11)}$$

4.7. the gravitational potential and the Geoid.

By virtue of its position in a gravitational field, a mass ' m' has gravitational potential energy. The energy can be regarded as the negative of the work done on ' m' by the gravitational force of attraction in bringing m from infinity to its position in the field. The gravitational potential V is the potential energy of m divided by its mass. Because the gravitational field is conservative, the potential energy per unit mass V depends only on the position in the field and not on the path through which a mass is brought to the location.

To calculate V for the rotationally distorted model Earth, we can imagine bringing a unit mass from infinity to a distance r from the center of the model along a radial path.

Since g_m is a conservative field, it can be derived from V as

$$g_m = \nabla U \text{ and } \text{Curl } g_m = 0$$

$$U = \int_r g_m .\, dr = - \int_\infty g_m .\, dr = \int_\infty g_m .\, dr$$

$$U = \int_\infty [\, GM/r'^2 - 3GMa^2J_2 / 2r^4 (3\cos^2 \phi - 1)\, dr$$

$$\mathbf{U = -GM/r + 3GMa^2J_2 / 2r^3 (3\sin^2 \phi - 1)} \qquad \mathbf{(4.12)}$$

In evaluating U, we assume that the potential energy at infinite distance from the Earth is zero. The gravitational potential adjacent to the Earth is negative; the Earth acts as a potential well. The first term in the above equation is the gravitational potential of a point mass. It is also the gravitational potential outside a spherical symmetric mass distribution. The second term is the effect on the potential of the Earth model' s rotationally induced oblatness. A gravitational equi- potential surface is a surface on which V is a constant. Gravitational equipotential are spheres for spherically mass distribution.

4.7.1 Gravity Potential (U).

The gravity potential accounts for both mass gravitation and rotation of the model Earth.

$$U(r, \phi) = -\int g .\, dr' = \int_\infty GM/ r^2 - 3GMa^2J^2 /2r^4$$
$$(3\sin^2 \phi - 1) - \omega^2 r' \cos^2 \phi)$$

$$\mathbf{U(r, \phi) = - \int GM/ r^2 + Gma^2J_2 / 2r^3 (3 \sin^2 \phi - 1) - 1/2\, \omega^2 r^2 \cos^2 \phi} \mathbf{(4. 13)}$$

A gravity equipotential is a surface on which U is a constant. Within a few meters the surface defines an equipotential surface. Therefore, elevation above or below sea level are distances above or below a reference equipotential surface.

The reference equipotential surface that defines sea level is called the Geoid. We now obtain an expression for the geoid surface that is consistent with our second order expansion of the gravity potential in equation above.

U at the equator - ($\phi = 0$, $r = a$)

$$U_0 = -GM/ a + Gma^2J_2 / 2a^3 [3\sin^2 \phi - 1] - 1/2 \omega^2 a^2\cos^2 0.$$

$$\mathbf{U_0 = -GM /a [1 + 1/2 J_2] - 1/2 \omega^2 a^2} \qquad \mathbf{(4.14)}$$

The value of the surface gravitational potential at the poles must also be U0, since we define the surface of the model Earth to be an equipotential surface.

Here $r = b$ and $\phi = -\pi/ 2$

$$U_0 = -GM/ b + Gma^2J_2 / 2b^3 (3\sin^2 90 - 1) - 1/2 \omega^2 b^2 \cos^2 90.$$

$$\mathbf{U_0 = -GM/ b [1 - (a/b)^2 J_2]} \qquad \mathbf{(4.15)}$$

The flattening (ellipcity) of the geoid is defined by:

f =(Equatorial radius - Polar radius)1/ equatorial radius

$$\mathbf{f = (a - b) (1/a)} \qquad \mathbf{(4.16)}$$

As expressed above;

U_0 AT THE EQUATOR = U_0 AT THE POLES.

$$\mathbf{-GM /a [1 + 1/2 J_2] -1/2 \omega^2 a^2 = -GM / b [1- (a/b)^2 - J_2}$$

multiplying through out by - a/ GM we have:

$$\mathbf{1 + 1/2 J2 + \omega^2 a^3 / 2GM = a/b [1 - J_2 (a/b)^2]}$$

Substituting b = a(1 -f) and neglect quadratic and higher order terms in f and J_2 (since f << 1 and J_2 << 1) we can have the final expression for f as shown below.

$$\mathbf{f = 3/2 J_2 + \omega^2 a3/ 2GM} \qquad \mathbf{(4.17)}$$

Taking $a^3 \omega^2 / GM = 3.46775 \times 10^{-3}$ and the satellite value

$$J_2 = 1.0827 \times 10^{3};$$

$f = 1/298.256$ is the ellipticity.

This is valid only if the surface of the planetary body is an equipotential. The shape of the model geoid is nearly that of a spherical surface; that is, if r_0 is the distance to the geoid,

$$r_0 \approx a(1- \varepsilon) \text{ where } \varepsilon << 1.$$

By setting $U = U_0$ and $r = r_0$ in the gravity potential equation and substituting the gravity potential at the equator for U_0 and $r_0 = a (1 - £)$, and neglecting quadratic and higher order terms in f, $J_{2,,}$ $a^3 \omega^2 /GM$, and e we obtain:

$$\varepsilon = [3/2 J2 + \omega^2 a^3 / 2GM) \sin^2 \phi \quad (4.18)$$

$$r_0 = a(1- \varepsilon) = a[1- (3/2J_2 + a^3\omega^2/2GM)\sin^2 \phi]$$

$$r_0 = a[1-f\sin^2 \phi] \quad (4.19)$$

where $f = 3/2 J_2 + a^3 \omega^2 / 2GM.$

The non-dimensional quantity $a^3\ \omega^2$ /GM is a measure of the relative importance of the centrifugal acceleration due to the rotation of the Earth compared with the gravitational attraction of the mass in the Earth. The rotational contribution is about 0.33% of the mass contribution.

In the above analysis we have considered only terms linear in J_2 and $a^3\ \omega^2$ / GM. In order to provide a reference geoid against which geoid anomalies are measured, it is necessary to include higher-order terms. By convention, the reference geoid is a spheroid (ellipsoid of revolution) defined in terms of the equatorial and polar radii by:

$$(r_0 \cos \phi)^2 / a^2 + (r_0 \sin \phi)^2 / b^2 = 1$$

The eccentricity of the spheroid is given by:

$$e = (a^2 - b^2)^{1/2}\ l/a = [\ 2f - f^2]^{1/2}$$

Using b = a (1 - f) in the spheroid equation and simplifying for r_0 gives:

$$\mathbf{r_0 = a\ [\ 1 + (2f - f^2) / (1 - f)^2\ (\sin^2 \phi)\ ]^{-1/2}} \qquad \textbf{(4. 20)}$$

If this equation is expanded in powers of f and if terms of quadratic and higher order in f are neglected, the result is in agreement with $r_0 = a (1 - f \sin^2 \phi)$.

With a = 6378.139km and f = 1/ 298.256 defines the reference geoid.

The difference in elevation between the measured geoid and the reference geoid ΔN is refereed to as a geoid anomaly. The maximum geoid anomalies are of the order of 100m; this is about 0.5% of the 21km difference between the equatorial and polar radii. The largest geoid anomaly is the negative geoid anomaly off the southern tip of India ,which has an amplitude of 100m. No satisfactory explanation has been given for this geoid anomaly that has no surface expression. A similar unexplained negative geoid anomaly lies off the west cost of N . America.

The anomaly in the potential of the gravity field measured on the reference geoid ΔU can be related directly to the geoid anomaly ΔN. The potential anomaly is defined by:

$$\Delta U = Um_0 - Uo$$

Where U_{m0} is the measured potential at the location of the reference geoid and U_0 is the reference value of the potential defined by gravity potential at the equator. The potential on the measured U_0, as shown below. It can be seen from the figure that U_0, U_{m0} and U_N are related by,

Where Um_0 is the measured potential at the location reference value of the potential defined by gravity potential at the equator. The potential on the measured is U_0, as shown below. It can be seen from the figure that U_0, Um_0 and $\underline{U_N}$ are related by;

$$U_0 = Um_0 + (\delta U/ \delta r)_{r=r0} \Delta N, \text{ since } \Delta N/ a << 1.$$

It will be recalled from the derivation of gravity potential, that we obtained the potential by integrating the acceleration of gravity. Therefore, the radial of the potential in the above equation is the acceleration of gravity on the reference geoid. To the required accuracy we can write:

$$(\delta U/ \delta r)_{r=r0} = g_0$$

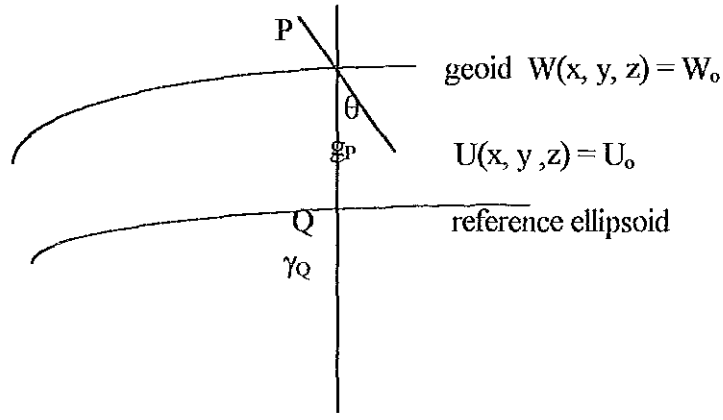

Fig. Relationship of measured and reference geoid and geoid anomaly ΔN.

$$U = U_{m0} + g_0 \Delta N$$

$$\Delta U = U_{m0} - U = -g_0 \Delta N$$

From the previous expressions we recall that:

$$\mathbf{g = GM/ r^2 - 3GMa^2 J_2 / r^4 (3\sin^2 \phi - 1) - \omega^2 r \cos^2 \phi} \qquad \mathbf{(4.21)}$$

Using the relations obtained in the preceding sections

$r = a [1- (3/2 J_2 + a^3\omega^2/ 2GM) \sin^2 \phi]$in equation (2.21) and neglecting quadratic and higher order terms as usual in the simplification ,one finds:

$$\mathbf{g_0 = GM/ a^2 [1 + 3/2 J_2 COS^2 \phi] + a \omega^2 [sin2 \phi - cos^2 \phi]} \quad \mathbf{(4. 22)}$$

N.B. To provide a standard reference acceleration of gravity against which gravity anomalies are measured, it is necessary to retain higher order terms which are not treated in the above expressions.

By letting U =U_0 and r = r_0 and neglecting quadratic and higher order terms in f, J_2, a^3 ω^2/GM and using r_0=a (1 - ε) we obtain:

$$\varepsilon = [\ 3/2\ J_2 + a^3\ \omega^2\ /\ 2GM\ ]\ \sin^2\phi$$

We find a model equation for the equipotential surface known as ellipsoid. i.e.

$$r_0 = a[1 - (3/2J_2 + a^3\omega^2/2GM)]\sin^2\phi = a[\ 1 - f\sin 2\ \phi\ ]$$

$(\delta U/\ \delta r\ )_{r=r} = \gamma$, is the theoretical gravity field on the ellipsoid (distorted earth model).

$$\gamma = GM/a^2\ [\ 1 + 3/2\ J_2\ COS^2\ \phi + \ a^3\ \omega^2\ (\ \sin 2\ \phi - \cos 2\ \phi\ )\ ]$$

$$\gamma \ = g_e\ [\ 1 + c_1\ \sin^2\ \phi + c_2\ \sin^2\ 2\phi\ ]$$

$$\gamma_{1967} = 978031.846[1 + 0.0052789\sin^2\ \phi - 0.000005\ \sin^2\ 2\phi\ ]\text{mGal}$$

This is the IGRS 1967 (International Geophysics Reference System) formula to calculate the theoretical gravity as a function of latitude (ϕ). For any point on the surface of the earth γ can be calculated as a function of latitude because;

- it is not symmetrical.

-mass distribution is not the same.

-and density distribution is not the same.

Gravity not only varies radially but it also varies laterally. This difference from the theoretical value we call it anomaly as it will be discussed later.

4.8.Gravity Data Reduction.

The basis on which gravity observations have been reduced to the **B**ouger anomaly has been standardised by International agreements. Those in current use are the 1967 International Gravity Formula (which replace that of the 1930) for the computation of theoretical gravity (Miter mayor ,1969) and the International Gravity Standardisation Net (IGSN 71) (Morelli ,et al., 1974) which establish the best estimates of total observed gravity at recognised base stations all over the world and eliminates the error of about 14mGal which become evident in the old Postdam Datum. This encourage the computation of absolute (rather than relative) Bouger anomalies.

Gravity data only become useful In the geologic sense when a gravity anomaly is calculated- usually the Bouger anomaly on land and the free air anomaly at sea. The gravity anomaly at any observation point may be defined as the difference at the point between the " theoretical gravity " calculated according to the prescribed formula and "

observed gravity " based on some International base station datum and corrected for all factors except density variations in the underlying geology.

To do this for stationary gravity observations it is necessary not only to determine the value of g at the site, but also determine the altitude above sea level and the latitude of the site. If the observations are made from a moving survey platform, it is also necessary to correct for the east ward component of the platform velocity and eliminate vertical acceleration due to the motion of the platform itself (Eotovos correction).

For simple observation on the land surface, a reading accuracy of ± 0.1lmGal or better was attained many years ago. Since that time the ingenuity of the gravity surveys has been tested in terms of (a) determining other survey parameters with comparable (or acceptable) accuracy, and (b) reducing the time and cost of the gravity survey operations. A comprise in accuracy has usually been struck on pragmatic (rather than scientific) grounds, which include the nature of the terrain to be accessed.

Because the earth is not a perfect square, the gravitational acceleration is not constant over the earth's surface (Tsuboi, 1983). The magnitude of gravity depends on latitude, elevation, topography of the surrounding terrain, earth tides and density variations in the subsurface. For any gravity data obtained in the field observations, it must be corrected for elevation, the influence of near by topography, and latitude.

4.8.1. Latitude Corrections

If the earth were a homogenous non-rotating sphere with the same vertical gradient everywhere, apart from local near surface density variations due to geological structures ,and if it were a perfectly smooth surface, then clearly all gravity variations over the

surface would be caused by geological structure. But this is not so. Because of the flattening, the poles are nearer to the center of mass than the equator, so the gravity increases with increasing in latitude. The variation of gravity with latitude over the surface of an ellipsoid earth can be expressed using the theoretical gravity formula (IGRS 1967). The latitude correction δg_L is obtained by differentiating the theoretical gravity formula and is added to g as we move towards the equator, i.e.

$$\delta g_L / \delta s = (1/ R) \delta \gamma_\phi / \delta \phi = 0.811 \sin 2\phi \text{ mGal /km} \qquad (4.23)$$

Where R = 6371km is the radius of the earth, &

$\Delta s = R\delta\phi$ = N-S horizontal distance, and ϕ is the latitude angle (Telford, 1990).

4.8.2. Free Air Correction.

Gravity varies with elevation . A point at higher elevation is farther away from the center of the earth and therefore has a lower gravitational acceleration than the one at lower elevation. The free air correction accounts for only changes of gravity with height. So it is necessary to correct for changes in elevation between stations to reduce observations to a datum surface (Tsuboi, 1983). The correction is obtained by differentiating the scalar equation for a spherical earth.

$$g = GM/ R^2$$

The gravity at a point located at a height h above the geoid is (Tsuboi, 1983)

$$g_h = GM/ (R+h)^2 = GM/R^2(1+ h/R)^2 = g(1+ h/R)^{-2}$$

Applying the Binomial expansion for the term $(1 + h/R)^{-2}$ and ignoring higher order terms by taking only the first two terms we have:

$$g_h = g (1 - 2h/R).$$

The free air correction is given by:

$$\delta g_{FA} = g - gh = 2gh / R = 0.3086mGal / m \qquad (4.24)$$

N.B. The free air correction is added to the gravity reading when the station is above the geoid and subtracted when below it.

4.8.3. Bouger Correction.

In the free air correction the attraction of any material between the station and a datum plane was ignored. It is the correction for the attraction as approximated by considering the material as an infinite horizontal slab. The gravity attraction for a point on the surface of a slab obtained by calculating the effect of an infinite disk is given by:

$$\delta g_B = 2\pi G p h$$

where h is the height of the gravity station above the geoid and

G is the gravitational constant.

For mean crustal density (2.67 gm/cm3) and h in meters, the Bouger correction reduces to:

$$\delta g_B = \mathbf{0.1119h\ mGals/m} \qquad \mathbf{(4.25)}$$

The Bouger correction (reduction) is applied in opposite sense to the free air correction ,i.e., it is subtracted when the station is above the geoid and vice-versa.

4.8.4. Terrain Correction.

The effects of surface irregularities in the vicinity of a station are accounted for by terrain correction. Though many methods exist for calculating terrain corrections, all of them require detailed knowledge of relief near the station and a good topographic map extending considerably beyond the survey area.

Terrain correction is done by computing graphically the gravity effect at the observation point of all the hills above the station level and all valleys below it. One such method is that of Hammer 91939): Specially designed transparent graticule is divided in to zones by circles, which being subdivided into compartments by radial lines. The total effect is

the sum of each compartment, which each compartment being computed by its average height. The gravity effect of a single sector is calculated from the formula.

$$\delta g_{sec}(r,\theta) = G \rho \theta [(r_0 - r_1) + (r_1^2 - h^2)^{1/2} - (r_o^2 + h^2)^{1/2}]$$

Where θ is the sector angle in radians, $h = | e_S - e_a |$, e_s is the station elevation, e_a is the average elevation in the sector, and r_0 and r_i are the outer and inner sector radii respectively. The terrain correction, δg_T, is the sum of all the contribution of the sectors.

$$\delta g_t (r,\theta) = \sum_r \sum_\theta \delta g_{sec}(r,\theta) \qquad (4.26)$$

There is another method of calculating terrain corrections using digital computers. This method of Kane (1962) use a scheme of digitising the topography by writing the elevations at points on a uniform grid so that the same grid points can be used for all stations.

4.8.5. Drift Corrections.

The null reading value of gravimeters change gradually with time. The main cause of this drift is a creep in the springs and is usually unidirectional. The correction is often made by connecting and finishing a set of observations at the same point having noted the time at which measurements were taken. The drift which is usually positive, is the difference between the last and the first observations. It is found to be proportional to time, which

means that the amount of drift to be substituted from all the observations taken over the period can be easily determined.

4.8.6. Earth Tide Corrections.

The variations of gravity result from external causes in addition to internal causes of drift. The gravitational attraction of the sun and the moon as their positions change with respect to the earth is the cause for this external tide. The corrections can be calculated from knowledge of locations of the sun and the moon. However, because the variation is smooth and relatively too low, usually it is included in the drift correction.

4.9 The Gravity Anomalies.

A gravity anomaly is any variation in gravity from a predicted computed value for the latitude corresponding to the station. Such anomalies are usually the primary data from which a geological interpretation of their source is attempted. In the geodetic sense the anomaly is a single numerical value for any individual observation and is the difference of the observed value from a theoretical or calculated value based on certain assumptions about the form of the gravity field over the earth as a whole.

4.9.1.Free Air Anomaly.

Only the effect of elevation of a station from the geoid is considered by the free air anomaly. Here the attraction of materials between the elevation and the sea level (the

geoid) will not be taken into account and that is why it is called the free-air. Thus, this free air anomaly is given by;

$$\Delta g_{FA} = g_{obs} + 0.3086h - \gamma_{\phi} \qquad (4.27)$$

4.9.2.Bouger Anomaly.

The Bouger anomaly is the difference between the measured value at the point of observation and the theoretical value calculated for that elevation or water depth, by considering a Bouger slab of appropriate density for the effect of Earth' s material between the geoid and the station. The Bouger anomaly calculated by ignoring topographic effects is known as simple bouger anomaly .

$$\mathbf{S.B.A.} = g_{obs} + 0.3086h - 0.1119h - \gamma \qquad (4.28)$$

When all corrections, the free-air, Bouger, together with the terrain correction are applied to the observed gravity, the resulting anomaly obtained by subtracting the standard theoretical gravity at the given latitude is called the Complete Bouger Anomaly (C.B.A.) and is given by:

$$\mathbf{C.B.A.} = g_{obs} + 0.3086h - 0.1119h + \delta g_t - \gamma \qquad (4.29)$$

CHAPTER 5

THE GRAVITY DATA

5.1 INTRODUCTION

The previous geophysical works discussed in chapter 3 were aimed at studying specific geological problems related to crustal and upper mantle structures of the Ethiopian rift system. The major objectives of the present research work is also reduction and preparation of all available gravity data and interpret the produced gravity maps in terms of the geologic and tectonic features of the study region, and compare the results obtained with the previous works aforementioned. Though a limited number of gravity observations were made under this survey, the task were accomplished with data compiled from different sources and reprocessed following the procedures in gravimetry as applied to geophysics.

5.2 DATA PREPARATION AND PROCESSING

Gravity measurements have been carried out in Ethiopia since 1960.The work was not intended in establishing a standard base station network but to study geological problems related to the crustal and upper mantle phenomena of the Ethiopian Rift System. For this reason the majority of the previous data acquired are distributed in the rift system particularly the Main Ethiopian Rift, the Afar depression and the associated rift shoulders. As a consequence of this there were major problems such as lack of first and second order gravity

base stations, lack of calibration lines to check the gravimeters used in the previous observations.

In accessibility of the rift shoulders, accuracy problem of altimeter heightening, terrain effects, absence of topographic maps at a scale of 1:50,000, ...etc.

Almost the majority of the data obtained from the EIGS and A.A.U. suffer from the effect of the above cited problems to a greater degree as compared to gravity observations made these days (e.g. the gravity observation under this survey).In addition to this the previous observations were tied to the Geophysical observatory gravity base station whose IGSN value (g = 977452.16 mGal). was known until recently and found correctly reported in Dr. Abera's PHD work (1992).

In most gravity survey reports and M.Sc thesis works based on this data of previous gravity surveys it is quoted that the datum value used to tie the observed values is IGSN71 datum when it actually is the potsdaam datum value (g = 977467.07). With the exception of a few data acquired recently and tied to the correct IGSN71 Datum value, the above misquotation of the datum value has resulted in heterogeneity in all gravity data acquired by the EIGS. The consequence of this heterogeneity has generated quite a considerable trouble in homogenising the data used in this study.

To alleviate this problem of datum inhomogenity corrections were made to the previous data obtained from the sources mentioned above using the following steps.

The **observed gravity** values from the previous surveys conducted in the study region, whose sources include:

-the Ethiopian institute of geological surveys (EIGS) and

-the geophysical observatory of A.A.U (Dr. Abera's Ph.D. work).

were checked whether they are connected to the IGSN71 datum or to the Potsdam datum with:

- reobservations made on previously observed identical stations in the study area and

-computations made on theoretical considerations using a computer program developed by Dr Abera. This program computes gravity anomalies using observed relative gravity values referred to the two datum's (IGSN and POTSDAM) with theoretical gravity (γ_ϕ) values calculated according to GRS1930 and GRS1967 and finally determines which particular observed gravity value is connected to which particular datum.

The measures taken above resulted in heterogeneity in datum for almost all the previous data obtained and this proved that the observed gravity values obtained from the EIGS were not available to the IGSN71 Datum; even if it was reported that they are tied.

Hence, reprocessing and re-evaluation of the previous data obtained from the EIGS became an inevitable task in order to keep the consistency between the two data sets.

Accordingly, all the previous data were reprocessed with ties made to the IGSN71 station of the Geophysical Observatory, theoretical gravity computed according to GRS67 formula and the standard corrections discussed in chapter 4 properly applied with a uniform density of 2.67gm/cm^3 to compute the Free-air and the Bouguer anomalies. Furthermore, the level of error of the computed pointed Bouger anomalies at each station is determined according to the scheme outlined in section 5.3 here below and is estimated at ± 2.8 mGal. The reduction process was performed using a FORTRAN program developed by Abera (1999).

Terrain corrections were made for about 150 stations obtained from EIGS, AAU and the 50 stations observed under this survey. An estimated error of about 2 mGal was considered due to neglect of terrain effect for the rest of the stations. This estimate was based a statistical value calculated along two traverses that cross the Aluto mountain (2335 m), rising about 700 m above the rift floor by Dr. Abera (1992). This value is thought to apply for all stations and treated as systematic error in computing the over all mean square error of the computed point gravity anomalies.

A compilation of the data sets between the defined latitudes resulted in a total of 587 gravity stations. All the gravity stations occupied have been referred to the IGSN71 (Morelli etal.,1971). The primary base station used was that of the Geophysical Observatory IGSN base station (977452.16 mGal) located at Addis Ababa University.

As one of the major objectives of this M.Sc. research is to establish a homogenised gravity data set in a standard format for the study area considered, this task is accomplished and ready for any future geophysical or geological use that involves gravity data

5.3 ASSESSMENT OF ERRORS IN THE GRAVITY ANOMALIES

The assessment, computation and evaluation of the errors involved in the computed point Bouguer anomalies are reported by Abera (1992, 1998) as given below.

In analysing the accuracy of computed point gravity anomalies it is necessary to appraise the accuracy of the method used in computing them, i.e., the completeness of the formula used and the correctness of the numerical values of the constants occurring in it (Abera, 1992). A

systematic error may be introduced in the computed Bouguer anomalies, for example by neglecting the correction for irregularities in the terrain (terrain correction).

It is also necessary to assess the effect of random and systematic errors of the parameters of the formula, the values of which are determined separately for each gravity point.

These include the errors involved in the determination of:

⋆ the observed value of gravity (observation error or measurement precision) at each station

⋆ the point elevations (elevation error) at each station

⋆ the geodetic latitude (latitude error)

⋆ the reduction density (density error) of the topographic masses above sea level used in the in the computation the Bouguer anomaly values at each station.

We know that the computation of the point Bouguer anomalies values, Δg_B, for each observation point is performed in accord with the formula:

$$\Delta g_B = g + 0.3086h - 0.04191\rho h + \delta g_t - \gamma \qquad (5.1)$$

The accuracy, $\sigma_{\Delta g}$, in the determination of the point Bouguer anomalies, Δg_B, is dependent on the precision in the determination (observation error) of the parameters g, h, ρ and ϕ, involved in the formula.

Since the values of g, h, ρ and ϕ are determined separately for each gravity point, the precessions (observation errors) σ_g, σ_h, σ_ρ and σ_ϕ in the determination of g, h, ρ and ϕ respectively are independent to each other (i.e., are uncorrelated).

The overall mean square error $\sigma_{\Delta g}$ of the gravity anomalies, is defined by

$$\sigma^2_{\Delta g} = \delta^2_{\Delta g} + s^2_{\Delta g} \qquad (5.2)$$

where $\delta_{\Delta g}$ is the standard error (due to random errors) and $s_{\Delta g}$ is the systematic error (bias) of the gravity anomalies, Δg_B.

The variance $\delta^2_{\Delta g}$, can be computed from the law of propagation of errors for uncorrelated observations according to the following scheme:

Since the Bouguer anomaly formula is a function of the parameters g,h,ρ and ϕ, its implicit functional form is given by

$$\Delta g = \Delta g(g,h,\rho,\phi) \qquad (5.3)$$

The differential of Δg is expressed as

$$d\Delta g = (\partial\Delta g/\partial g)dg+(\partial\Delta g/\partial h)dh+(\partial\Delta g/\partial \rho)d\rho+(\partial\Delta g/\partial\phi)d\phi = \delta_{\Delta g} \quad (5.4)$$

The partial derivatives on the right hand side of Equation (5.4) above are independently evaluated upon substitution of Δg by the Bouguer anomaly formula, $\Delta g_B = g + 0.3086h$ -

$0.04191\rho h - \gamma$. The individual contributions to the standard error, $\delta_{\Delta g}$, due to the random errors (unavoidable errors) that occur naturally in the process of measuring (observing, determining) the relative point gravity values, point elevations, point geodetic latitudes of the gravity stations and density of the topographic masses are modelled and evaluated as follows.

★ The first partial derivative of Eq (5.3) results in

$$(\partial\Delta g/\partial g)dg = (dg/dg)dg = dg = \sigma_g \qquad (5.5)$$

and corresponds to the measurement precision (observation error) of the observed gravity values evaluated as follows,

Actual field tests made with observations taken at 4 national base stations (check points) located in Addis and its environs (Table 1). Table 1 consists a summary of 12 independent observations made at 4 gravity check-points (national base stations), that means, 3 independent observations at each check point.

The measurement precision, σ_g, is obtained by computing the internal variance (Bjerhammer, 1973) of the 12 independent observations made at the 4 gravity check points following the scheme outlined in Table 1 and the formula:

$$\sigma^2_g = (\Sigma_{s1}(vv) + \Sigma_{s2}(vv) + \ldots + \Sigma_{s4}(vv)\}/(n\text{-}s) \qquad (5.6)$$

where n is the total number of independent observations, S1,S2...,S4 are the number of gravity check points, and v are residuals for the individual observations at each check point.

Table 1. Table of observed relative gravity values (mGal) for computing the internal variance of 12 independent observations taken at 4 check points.

	y	ŷ	v	vv	
S1:	1015.90	1015.92	-0.02	0.0004	$\Sigma_{s1}(vv) = 0.0078$
	1015.99	1015.92	0.07	0.0049	
	1015.87	1015.92	-0.05	0.0025	$\hat{y}_1 = 1015.92$
S2:	0994.99	0994.92	0.07	0.0049	$\Sigma_{s2}(vv) = 0.0083$
	0994.89	0994.92	-0.03	0.0009	
	0994.87	0994.92	-0.05	0.0025	$\hat{y}_2 = 0994.92$
S3:	1030.67	1030.69	-0.02	0.0004	$\Sigma_{s3}(vv) = 0.0078$
	1030.76	1030.69	0.07	0.0049	
	1030.64	1030.69	-0.05	0.0025	$\hat{y}_3 = 1030.69$
S4:	1027.71	1027.74	-0.03	0.0009	$\Sigma_{s4}(vv) = 0.0083$

1027.81	1027.74	0.07	0.0049	
1027.69	1027.74	-0.05	0.0025	$\hat{y}_4 = 1027.74$

Findings of this investigation indicate that the gravimeter has a measurement precision computed using Eq (5.6) above as,

$$\sigma_g = \pm [(0.0078 + 0.0083 + 0.0078 + 0.0083)/(12-4)]^{1/2}$$

$$= \pm 0.06 \text{ mGal}$$

$\sigma_g = \pm 0.06$ mGal is therefore, the computed observation error estimate (the overall reproducibility of the gravimeter) that one may encounter when taking readings with this gravimeter.

★ The second Partial derivative of Eq (5.3) results in,

$$(\partial \Delta g/\partial h)dh = d/dh(0.3086h - 0.04191\rho h)dh \qquad (5.7)$$

‣ By making use of the adopted reduction density, $\rho = 2.67$ g/cm^3 and the precision in the elevation determination, $\sigma_h = 10$ m, reported , the error introduced in the computed Bouguer anomalies due to elevation error is computed & amount to:

$$(0.3086\text{-}0.04191 \times 2.67)\sigma_h = \pm 1.97 \text{ mGal.} \quad (5.8)$$

★ The third partial derivative of Eq (5.3) results in,

$$(\partial\Delta g/\partial\rho)d\rho = d/d\rho(0.04191\rho h)d\rho \quad (5.9)$$

‣ Supposing that we want to achieve a reduction precision of 0.1 mGal in the Bouguer reduction using the Bouguer plate gravity formula given by

$$g_{BP} = 2\pi G\rho h = 0.04191\rho h \quad (5.10)$$

The precision of density determination, which is required for the computation of Bouguer anomalies follows as,

$$\sigma_\rho = d\rho = (1/0.04191h)dg_{BP} \quad (5.11)$$

For the mean elevation, $\hat{h} = 1869.15$ meters, of the of the gravity stations along the profile we considered in the determination of the reduction density, $\rho = 2.67$ g/cm^3, the precision of density determination would amount to,

$$\sigma_\rho = (1/0.04191 \times 1869.15) \times 0.1 = 0.0013 \text{ g/cm}^3 \quad (5.12)$$

The error introduced in the computation of the point Bouguer anomalies due to density error is therefore computed as,

$$(\partial\Delta g/\partial\rho)d\rho = (0.04191 \times \hat{h})\sigma_\rho = \pm 0.10 \text{ mGal} \quad (5.13)$$

★ The last partial derivative of Eq (5.3) results in,

$$(\partial\Delta g/\partial\phi)d\phi = 1/R(\partial\gamma/\partial\phi)d\phi \quad (5.14)$$

‣ By differentiating the expression for the normal gravity given by Equation (4.23), with respect to ϕ and letting R = 6371229m (mean earth's radius), the rate of change of the normal gravity with latitude is estimated by

$$1/R(\partial\gamma/\partial\phi) = 0.813 \sin 2\phi \text{ mGal/km} \quad (5.15)$$

For the mean latitude, $\phi \leq 8.37°$ of the study area, the variation in the normal gravity is about 0.00023 mGal for each meter travelled in a N-S direction. Thus for each meter error north or sou2th in the measured position of an observation site, an error of 0.00023 mGal (0.00023mGal/m) will be introduced in the value of γ.

For the precision estimate, $R\sigma_\phi = \pm$ 200 m, in the determination of the latitude (UTM co-ordinates) of the gravity stations scaled from 1:250,000 and 1:50,000 topomap, the error estimate in the normal gravity reduction for the computation of the Bouguer anomalies amounts to:

$$1/R(\partial\gamma/\partial\phi)R\sigma_\phi = 0.05 \text{ mGal (for } \phi \leq 8.37°) \quad (5.16)$$

The variance, $\delta^2_{\Delta g}$, which would now be expressed as

$$(\delta_{\Delta g})^2 = (\sigma_g)^2+(\partial\Delta g/\partial h)^2(\sigma_h)^2+(\partial\Delta g/\partial\rho)^2(\sigma_\rho)^2+(\partial\Delta g/\partial\phi)^2(\sigma_\phi)^2 \quad (5.17)$$

and the over all mean square error, expressed as

$$\sigma^2_{\Delta g} = \delta^2_{\Delta g} + s^2_{\Delta g}$$

$$= (\sigma_g)^2+(\partial\Delta g/\partial h)^2(\sigma_h)^2+(\partial\Delta g/\partial\rho)^2(\sigma_\rho)^2+(\partial\Delta g/\partial\phi)^2(\sigma_\phi)^2 + s^2_{\Delta g} \quad (5.18)$$

is computed upon substitution of the values evaluated using Eqs (5.6), (5.8), (5.13), (5.16) for each term on the right hand side of Eqn.(5.18) and amounts to

$$\sigma_{\Delta g} = \pm [(0.06)^2 + (1.97)^2 + (0.10)^2 + (0.05)^2 + 2^2]^{1/2} = \pm 2.8 \text{ mGal}$$

Since a systematic error, $s_{\Delta g}$=2 mGal is introduced in the survey process due to neglect of terrain correction, the overall mean square error, $\sigma_{\Delta gB}$, of the point Bouguer anomalies computed using Equation (5.1) amounts to the effect of the random errors and the systematic error and is estimated about ± 2.8 mGal.

5.4. THE GRAVITY ANOMALY MAPS

As a rule of thumb, the first step in the interpretation of a geophysical survey data is compilation of anomaly map of the area.

The computed Bouguer anomaly values are reported as Free - air anomaly map (Fig.5.2) and Bouguer anomaly map (Fig.5.3) by plotting them on 1:250,000 scale map of the study area. The contouring is made in 5 mGal (CI) isoanomaly curves. The task is performed using the standard gravity and magnetic mapping software, Geosoft (1996) on a gridded data with a grid cell size of 0.05 and default blanking distance.

With very few exceptions, the stations exhibit consistent trends of the gravity values, thus demonstrating the overall good quality of the survey.

The judgement made on the quality of the survey and the choice of the contour interval (CI = 5 mGal) employed in the compiled Bouguer anomaly map are based on the level of error of the point Bouguer anomalies determined in section 5.2 and estimated at ± 2.8 mGal.

Furthermore, the separation of the regional effect from the Bouguer anomaly was performed using a computer program based on the trend surface of the regional gravity anomaly approximated using a polynomial surface fitting of degree 2. The corresponding residual

anomalies were then obtained, and using the same square grid interpolation, the regional anomaly map (Fig.5.5) and residual anomaly map (Fig.5.4) are produced. Preliminary qualitative interpretation of these maps has been made using as a constraint, the geological and / or structural map (Fig.2) of the MER, compiled by G.M. DI Paola (1972), and the results of previous geophysical surveys

5.4.1. FREE - AIR ANOMALY

There is a close correlation between the pattern of the free air anomaly (Fig.5.1) and the topography of (Fig.5.2) the study region. However, an overall correlation can not be obtained between the anomalies and the subsurface geological and structural features. Thus, it is limited to support in the interpretation of the Bouguer anomalies.

The free air anomaly values vary from -50 to 70mgals within the study area. The highest value of the anomaly occurred at the NW part of the survey area with an amplitude of 70 mGal with the highest elevation 2989m around Mt. Ziquala. The other maximum value of 50 mGal occurred on the NE plateau around Areb Gebya with an elevation ranging up to 2500m. On the SW part, a low free air anomaly (-50Mgal) occur.

The curvilinear nature of the main Ethiopian rift at about 8°N latitude is clearly evident. The free air anomaly map also reveals the E-W structural trend which is evident in other anomaly maps. This may be due to the presence of en echelon faults.

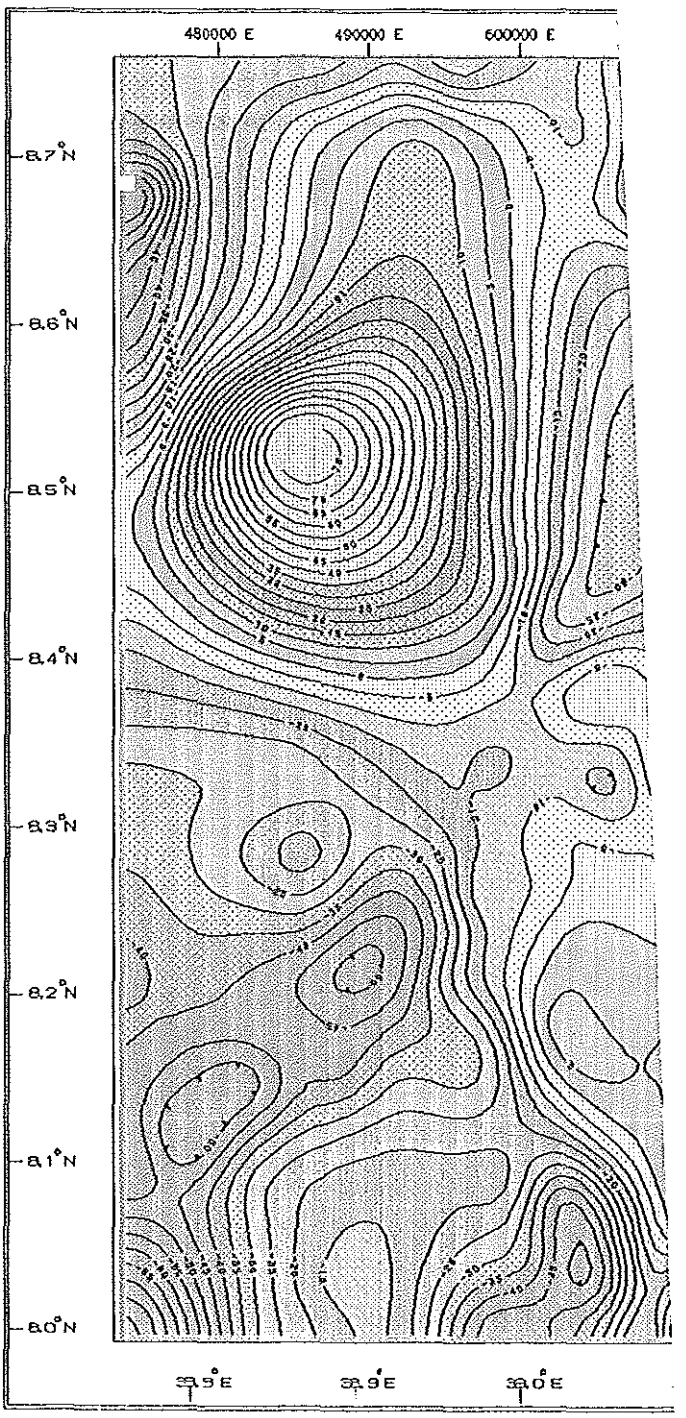

Fig 5.1 FREE AIR ANOMALY MAP OF GEDEMSA AND ITS AD

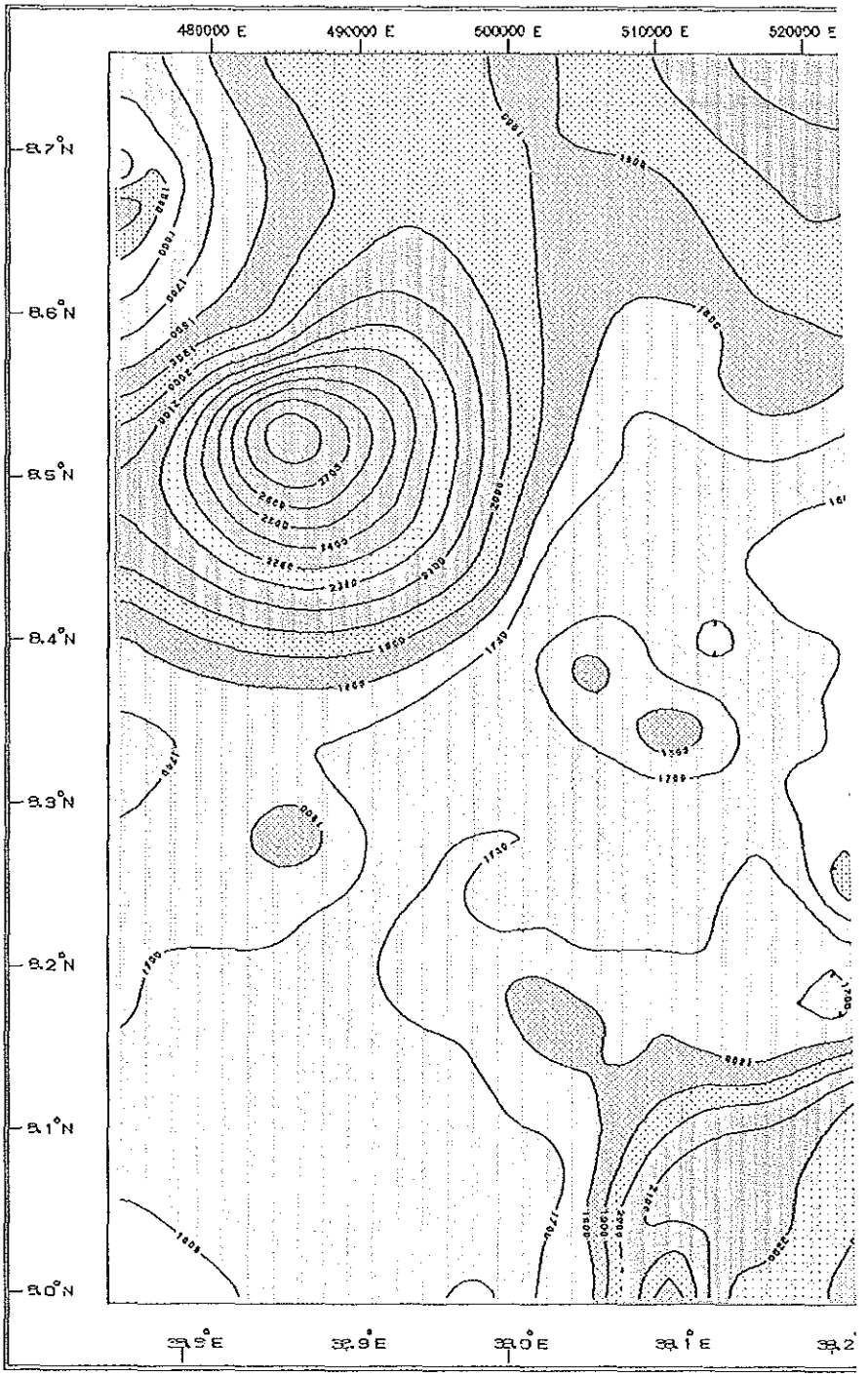

Fig 5.2 ELEVATION CONTOUR MAP OF GEDEMSA AND ITS ADJACENT AREA, CO

5.4.2 BOUGUER ANOMALIES

The Bouguer anomaly map produced (Fig.5.3) reveals an overview of the topographic feature and underlying crustal structures. The distinction between the rift and the adjacent plateaus and the regional structure features were depicted from the map on the basis of the general shape and wavelengths of the anomalies. However, anomalies on the Bouguer map have no great significance on the structural and geological features of shallow origin. Separation of the regional and residual anomalies from the Bouguer gravity map and their qualitative interpretation led to defining the anomalies related to deep structures, and local anomalies of shallow origin respectively.

The positive anomaly is the effect of both near surface and deep seated anomalous materials. The adjacent negative anomalies may be a description of low density volcanics on the surface or low density upper mantle material beneath the surface .The boundary between the rift floor and both the eastern & western escarpments are clearly marked by the bouger anomaly map.

As shown in the previous works of Mohr and Gouin (1967,68) the rift valley is in gravity 'low'. The broad negative anomaly of the rift shown on the Bouguer map trends approximately N-S between latitudes 8.00^0 and 8.750N and curves to NNE-SSW orientation towards the Afar depression. A series of local positive and negative anomalies are superimposed on the broad negative anomaly which are related to local variations in geological structure.

Bouguer gravity values are closely related to the morphological features. The present work shows gravity minima which are located in areas of maximum elevation around Areb gebya along the main road to Asela (Z7). The minimum gravity anomaly with amplitude of -

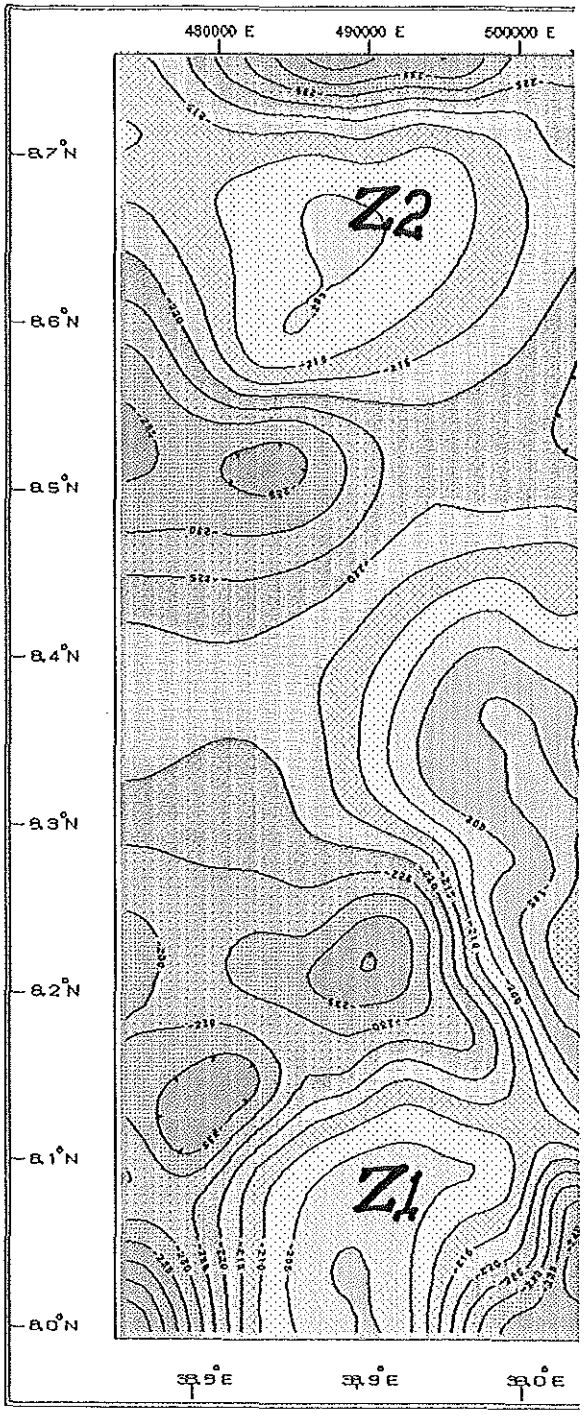

Fig 5.3 BOUGUER ANOMALY MAP OF GEDEMSA ANI

250Mgals occur in the SE part (Z7). Other local minima ranging between -245 and-205mgals are also located on the NE plateau adjacent to Nazret. The eastern plateau is also marked by a gravity 'low' with a minimum value of -210mgals.

On the central part, the intensity of gravity ranges from -185mgal in the main Ethiopian rift and increases to -140mgal towards NE which is a depression area East of Nazret with an elevation ranging from 1300-1600m above sea level (See Z4).The central positive anomaly zone (Z5) is associated to gedamssa and its surroundings. The other positive anomaly zone (Z6) corresponds to a depression area South of Haro Robi. The positive anomaly zone (Z6) in the SW of the area is a region adjacent to Lake Zeway. The pattern of a series of anomaly belts separated by small gravity highs show the general trend of the rift axis. The other positive anomaly zone (Z2) in the NW of the map is the area located North of Mt. Ziquala & South of Debre zeit town. On the southern part of the anomaly map there is a clear structural trend (NE-SW) which separate the high and low anomaly values between the depression and the elevated areas (see Fig.5.3).

Gravity gradient increases eastward from the western border and reaches maximum at the boundary of the eastern Ethiopian plateau. The negative anomaly in the SE corner of the area is due to the presence of low density materials such as ash flow tuffs, pantelliric ignimbrites and unwelded tuffs (the so called the Nazret group).

5.4.2.1. Residual Anomalies

The residual gravity map (Fig.5.4) characterises the general pattern of the Bouguer map, but with small local anomalies appearing after the removal of the regional. Particularly, the

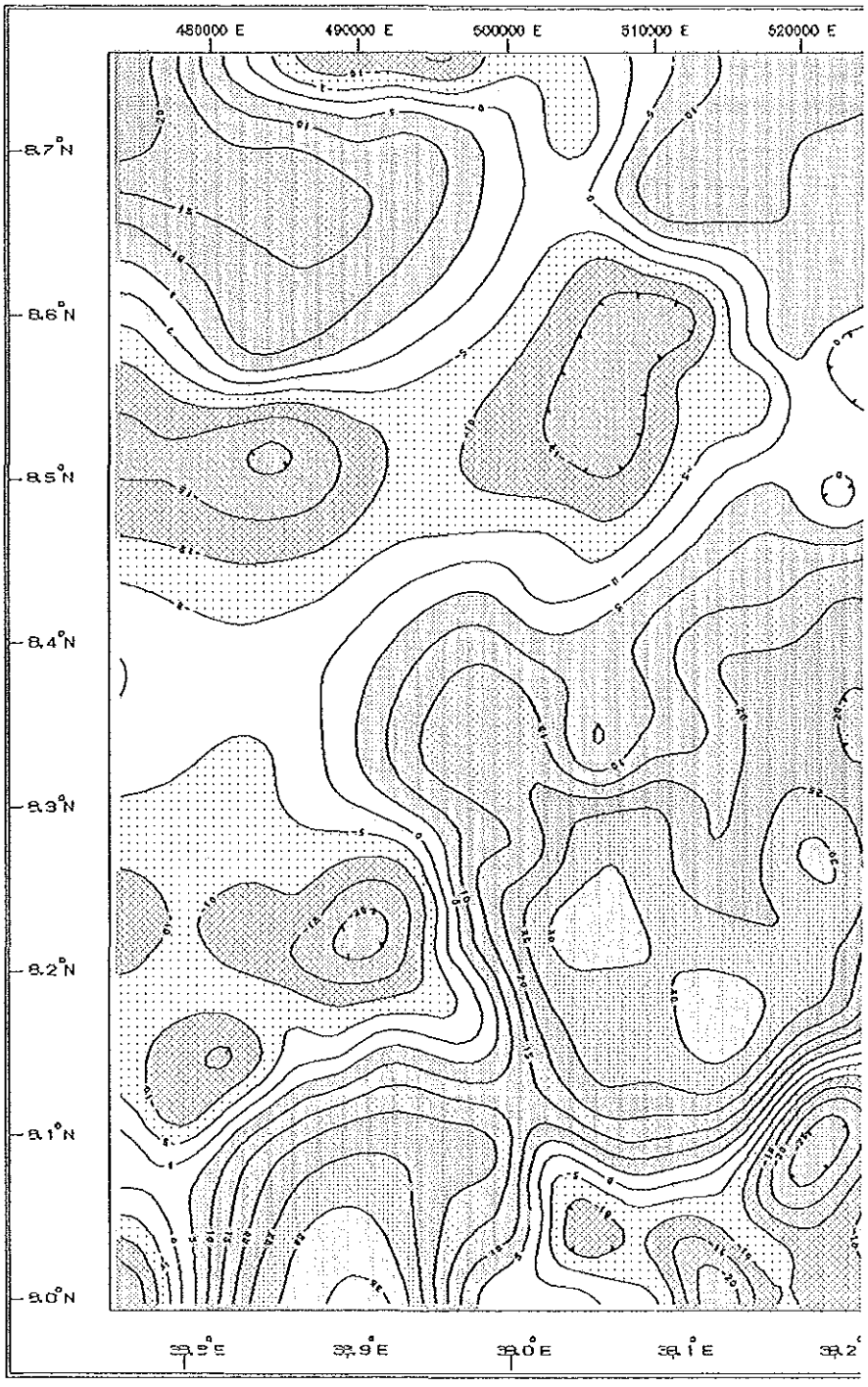

Fig5.4RESIDUAL BOUGUER ANOMALY MAP OF GEDEVSA AND ITS ADJACENT

Bouguer map shows a trend of elongated maxima running northwards parallel to the main escarpment, with increasing values, which this according to Makris and Ginzburg (1985) was associated with the crustal thinning towards the coast of the Red sea.

There is a high residual bouger anomaly trending SW-NE which are clearly observed in the Bouger anomaly map. This is an indication that the intense positive anomalies along the rift trend are near surface effects. This may be due to the regional structural feature, such as the Wonji fault, regional rift trending i.e. NNE-SSW. These enhancing features clearly indicates the continuation of the rift trend NE-SW .The fissural lavas of basic and intermediate composition may be the cause of this observed anomaly.

There is also a sharp E-W trending boundary, with a gravity low anomaly in the northern side and relatively high gravity anomaly in the southern part. This may be due to the presence of en echelon faults.

There is an intense positive anomalies in the rift trend described above. These intense positive anomalies are found to be associated with the axial zones of recent faulting (WFB),volcanism, and geothermal and seismic activity .

There is a wide zone of negative bouger anomaly (Fig.5.4)(short wave length anomaly trending from E-W to NNE broadening at the western side. This may be correspond to marginal grabens appear to run along the whole length of the west side of the rift floor.

There is also a spot -ve anomaly in the extreme south and SE corner of the study area, where as a similar spot positive anomaly are observed in the extreme north and NW of the area.

5.4.2.2. REGIONAL ANOMALY

The regional anomaly map (Fig.5.5)which was extracted from the Bouguer map shows smoothed large scale regional features. It indicates gravity minimum on the eastern plateau increasing values towards the west with the minimum value being located roughly Southwest of the study region. The regional anomaly indicates a gravity low in S-SW and gravity high in the N-NE which might probably related to the events of the rift flooring (basaltic rocks) and to the rift shoulder high topographic rocks. This causes the thinning the continental crust towards the direction of the rift flooring.

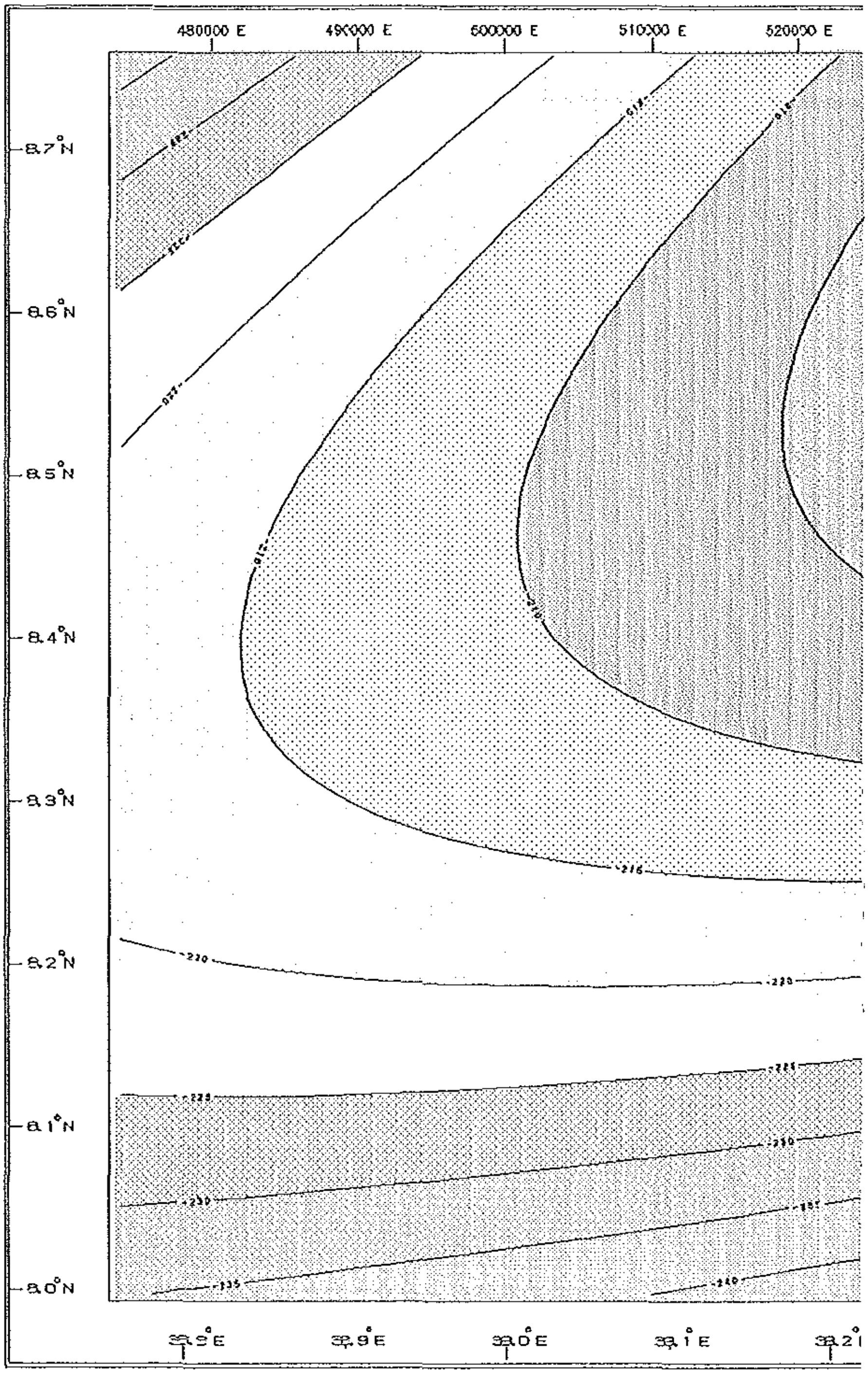

Fig5.5 REGIONAL BOUGUER ANOMALY MAP OF GEDEMSA AND ITS ADJACENT

CHAPTER 6.

DISCUSSIONS, CONCLUSIONS AND RECOMMENDATIONS

6.1. DISCUSSION

The gravity data, reduced to the IGSN71 datum, is presented in a standard format as one of the objectives of this thesis work is so. The availability of this data will provide researchers with a considerable information of the gravity field of the study region

and could be applied for further research programs intended to be conducted in the region.

A qualitative interpretation of the compiled Bouguer map, using the existing geological information, revealed the inverse correlation between the topographic relief and the Bouguer anomalies. local minima and maxima superimposed on the broad negative regional anomaly show the existence of structural units having density contrasts with the surrounding. The existing geological features and some isolated structural units identified in the previous works are further confirmed.

6.2. Conclusions

The main conclusions are:

-The long wavelength negative Bouguer anomalies that characterise the regional structure is disturbed by the relatively high anomaly belt

-The regional gravity values are related with the deep structural features. The pattern of the isogal anomalies on the regional anomaly map indicate the transition from the plateaus with higher Bouguer masses above sea level, towards the Red sea via the Afar depression. The

Afar depression is probably very attenuated continental crust, forming a platform between continental and oceanic rifts.

-Part of the Ethiopian dome is located on the western plateau at about the latitude of Addis Ababa. It is marked by minimum regional anomaly indicating the existence of a low density material beneath the crust.

-The existence of axial high anomaly belt along the Wonji fault belt, its extension towards central Afar following the fault belt and its occurrence coinciding with recent silicic volcanoes of the rift is further confirmed.

Compilation of the regional and residual anomalies from the Bouguer gravity map and their qualitative interpretation led to defining the anomalies related to deep structures, and local anomalies of shallow origin respectively.

As shown in the previous works of Mohr and Gouin (1967,68) the rift valley is in gravity 'high' as compared to the plateaus. The relatively positive anomaly of the rift shown on the Bouguer map strikes approximately NNE-SSW between latitudes 8^0 and 8.75^0N and curves to NE-SW orientation towards the Afar depression. A series of local positive and negative anomalies are superimposed on the relatively positive anomaly which are related to local variations in geological structure.

In general, there seems a close correlation between the Bouguer field and topography of the study region, where minimum gravity values are located in areas of maximum elevation and vice versa. The minimum gravity value with amplitude of -250 mGals occur around Areb gebya. Other local minima with amplitudes between -250 and -210 mGals are located on the

S& E plateau. The eastern plateau is also marked by a gravity 'low' with a minimum value of -250 mGals.

On the study region considered here, the intensity of gravity increases from -250mgal in SW & SE to -140mgal in the NE The pattern of a series of anomaly belts separated by small gravity highs show the general trend of the rift axis, following the axis of the Wonji fault belt. Gravity gradient increases eastward from the western border around Lake Zeway and decreases as we go towards east between 800000-900000m N.

The residual gravity map (Fig.5.4) characterises the general pattern of the Bouguer map, but with small local anomalies appearing after the removal of the regional.

A wide positive anomaly belt occur on the NE part following the rift trend. In the western escarpment adjacent to the main Ethiopian rift about 38.75^{0}E longitude, and gravity values decrease slowly towards the top of the western margin and then rise up slowly towards the rift floor where local anomalies are mainly related to rift volcanic centers and associated rocks.

The rift lakes basin is limited north by the uplifted Meki - Awash watershed and south by the upwarped margin of lake Shalla. The gravity gradient shown on the residual map, Northeast of lake Zway, confirms the important Meki - Awash watershed 'transverse arch' probably accompanied by shallow depth as interpreted by Gouin and Mohr (1964).

6.3 Recommendations

Based upon the investigations made under this study the following recommendations are forwarded.

1) All the previous gravity data collected by the EIGS & Other concerned Agencies have to be checked for their tie to an appropriate datum (IGSN71 Datum) in order to be homogenisely compiled in a standard format for reliable use by researchers in the Country.

2) Integrated geophysical work such as refraction seismic, reprocessing & interpretation of previous data collected in regions adjacent to the present study area is essential since these areas are a potential source for the economic development of the Country.

REFERENCES

Abera, A., 1983. Crustal Modeling from Gravity Data in the Ethiopian Rift. Ms. Thesis, Addis Ababa University, Addis Ababa, Ethiopia.

Abera, A., 1988. Gravity Field Interpretation Over the Main Ethiopian Rift. Proceedings of the 6th International Symposium "Geodesy and Physics of the Earth", Potsdam, Part II, pp. 99-115.

Abera, A., Sj`berg, L.E., 1990. Gravity Field Interpretation and Crustal Model Studies in the Main Ethiopian Rift. Presented at the Third International Symposium on Recent Crustal Movements in Africa. 8-16 December 1990, Aswan, Egypt.

Abera, A., 1992. The Gravity Field and Crustal Structure of the Main Ethiopian Rift. Ph.D. Thesis, Royal Institute of Technology, Department of Geodesy, Report No. 26 (TRITA GEOD 1026), Stockholm, Sweden.

Abera, A., 1998. The Gravity Survey of the Tana-Beles Hydroproject Tunnel Site. A Geotechnical report submitted to the Aquatech Pvt. Ltd. Company, Addis Ababa, Ethiopia (unpublished).

Abera, A., 1999. An interactive FORTRAN program that checks the datum that an observed relative gravity is tied to and computes the point Free-air and Bouguer anomaly values of a station.

Baker, B.H, Mohr, P.A. and Williams, L.A.J., 1972. Geology of the East Rift System of Africa. Geol. Soc. Am., Spec. Pap., 136:67pp.

Bjerhammar, A., 1973. Theory of errors and generalized matrix inverses. Elsevier Scientific Publishing Company, Amsterdam

Dereje, 1994. Volcanology, Petrology and Geochemistry of Gedamsa Volcano. MSc Thesis. Addis Ababa University, Addis Ababa.

Dobrin, M.B.,and Savit, C.H., 1988. Introduction to Geophysical prospecting. McGraw-Hill Inc. Singapore.

Gerland, G.D.,1979. Introduction to Geophysics-Mantle, Core and Crust, W.B. Saunders company, Philadelphia.

Ebinger, C., 1991. Southern Ethiopia Rift Gravity 2surveys: Interim Report to the Ethiopian Institute of Geological Surveys. Leeds University Dept. of Earth Sciences.

Falcon, N.L., Gass, I.G, Girdler, R.W. and Laughton, A.S.(Editors), 1970. A discussion on the structures and evolution of the Red Sea , Gulf of Aden and Ethiopian rift junction. Phil. Trans. R. Soc. London, Ser. A, 267: 1-417.

Gibson, I., L., 1967. Preliminary account of the volcanic geology of Fantale, shoa: Bull. Geophys. Obs. Addis Ababa, no. 10, p. 59-67.

Gibson, I., L., 1970. Quaternary pantelleritic volcanism in the Main Ethiopian rift: Univ.Leeds, Dept. Earth sci., 14th Ann. Rept. Research Inst. Africa Geol., p. 35-38.

Girdler, R.W., Fairhead, J.D., Searle, R.C. and Sowerbutts, W.T.C., 1969. The Evolution of Rifting in Africa, Nature, 224: 1178-1182.

Heiskanen, W.A. and Moritz, H., 1967. Physical Geodesy, Freeman, San Francisco.

Heman, S., 1939. Terrain corrections for gravimetric survey, Geophysics, Vol.4, No3, p184.

Makris, J., Menzel, H., and Zimmermann, J., 1972. A preliminary interpretation of the gravity field of Afar, northeast Ethiopia. In: R.W. Girdler (editor), East African Rifts. Tectonophysics 15 (1/2), 31-39.

Makris, J., Menzel, H., Zimmermann, J. and Gouin, P., 1975. Gravity Field and Crustal Structure of North Ethiopia. In: A. Pilger and A. R`sler (editors), Afar depression of Ethiopia. Stuttgart (Schweizerbart), 1: 135-144.

Makris, J. and Ginzburg, A., 1987. The Afar Depression: Transition between continental rifting and sea floor spreading. Tectonophysics, 141: 199 - 214.

Marsden, G. Southern Ethiopian Rift Gravity Surveys. (unpublished)

Mohr, P.A., 1960. Report on a geological excursion through southern Ethiopia: Bull. Geophys. obs. Addis Ababa, no. 3, p. 9-20.

Mohr, P.A., 1962. Surface cauldron subsidence with associated faulting and fissure basalt eruptions at Gariboldi pass, shoa Ethiopia: Bull. volcanol., v. 24, p. 421-428.

Mohr, P.A., 1967a. The Ethiopian rift system: Bull. Geophys. Obs. Addis Ababa, no. 11, p. 1-65.

Mohr, P.A., 1967c. Major volcano-Tectonic lineament in the Ethiopian rift system: Nature, v. 213, p. 664-665.

Mohr, P.A., 1968. The cenozoic volcanic succession in Ethiopia: Bull. volcanol., v.32, p. 5-14.

Mohr, P.A., 1971a. The Geology of Ethiopia: Haile Sellassie I university press, p. 161-164.

Torge, W., 1989. Gravimetry, Walter de Gruyter & Co., Berlin, Germany.

Wolde Gabriel, G., and Aronson, J.I., 1987. Chow Bahir rift: "A failed" rift in Southern Ethiopia: Geology, v. 15 p. 430-433.

Wolde, B., 1989. Cenozoic volcanism and rift development in Ethiopia. Journal of African Earth Sciences, vol.8, No.1,pp.99-105.

Woolard, G.P., 1959. Crustal structure from Gravity and Seismic Measurements. Journal of Geophysical research; vol. 64; no.10; pp. 1521-1544.